Mon. Not. R. Astron. Soc. **000**, 000–000 (0000) Printed 30 March 2016 (MN LATEX style file v2.2)

Halo Definition and Environmental Effects

Antonio S. Villarreal,[1⋆] Andrew R. Zentner,[1†] Christopher W. Purcell,[2‡] Andrew P. Hearin,[3§] and Frank C. van den Bosch[3¶]
[1] *Department of Physics and Astronomy & Pittsburgh Particle Physics, Astrophysics, and Cosmology Center (Pitt-PACC), University of Pittsburgh, Pittsburgh, PA*
[2] *Department of Physics and Astronomy, West Virginia University, Morgantown, WV*
[3] *Department of Astronomy, Yale University, Hew Haven, CT*

In preparation

ABSTRACT
Recent work has shown the importance of environment to the properties of dark matter halos. This brings conflict to standard implementations of the halo model and excursion set theory which assume that the properties of a population within the halo is determined by the mass of the halo alone. We seek to find a definition of the size of a halo that allows us to minimize the impact of assembly bias on halo model calculations. We analyze the dependence on environment of our properties using the method of marked correlation functions for several different halo definitions, utilizing the Diemer & Kravtsov (2015) simulations. We find that environmental dependencies are dramatically different as we vary the definition of the halo radius in terms of the overdensity Δ. At large length scales, we find that the majority of assembly bias is removed through suitable redefinition of Δ. We are able to determine that the majority of the reduction in assembly bias is related to the elimination of host halos that would cease to be hosts in catalogs at lower values of Δ. Further, we analyze how different mass cuts affect this methodology. We note that unresolved halos leads to assembly bias being missed and that the most massive halos seem to exhibit minimal assembly bias. We further note that the choice of halo definition can induce assembly bias and consider how this may be interpreted in the context of previous results in the literature.

Key words: cosmology: dark matter – cosmology: large-scale structure of Universe – galaxies: formation –galaxies: halos – methods: numerical

[ARZ: We should add Andrew Hearin and Frank van den Bosch. Look into formatting the title correctly. Once I'm happy with the quality of the writing, we'll also need to send this to Benedikt Diemer and Andrey Kravtsov and offer them authorship.]

1 INTRODUCTION

[ARZ: We will need to work on the introduction considerably as we get a better handle on the final results. The first two paragraphs can probably be combined into a single shorter paragraph. I also like to end the first paragraph by telling the reader what it is that we aim to do in the paper. The rest of the introduction will need be be completely rewritten in a more professional manner. However, let's get the middle of the paper complete before we work a lot on the introduction and conclusion sections. Please pay close attention to your wording. As an example, it is MUCH preferable to say "galaxies and clusters form within merging dark matter halos" than it is to say "the creation of observed galaxies and clusters is often seen as arising from the hierarchical mergers of dark matter halos." The second option is just too long-winded without adding any

⋆ E-mail: asv13@pitt.edu
† E-mail: zentner@pitt.edu
‡ E-mail: cwpurcell@mail.wvu.edu
§ andrew.hearin@yale.edu
¶ frank.vandenbosch@yale.edu

information.] [ASV: I think I've merged the first two paragraphs well, but I am uncertain if there is sufficient background at this point.]

In the concordance cosmology, galaxies and clusters form within merging dark matter halos(White & Rees 1978; Blumenthal et al. 1984). Being able to model the properties of dark matter halos and the galaxies within gives us a probe for the physical processes that go into galaxy formation. The excursion-set formalism of galaxy clustering (Bond et al. 1991; Lacey & Cole 1993; Somerville & Kolatt 1999; Zentner 2007) and the standard halo model of galaxy clustering (Seljak 2000; Peacock & Smith 2000; Scoccimarro et al. 2001; Berlind & Weinberg 2002; Bullock et al. 2002; Cooray & Sheth 2002) are two such methods, but rely on underlying asumptions. The first is that the statistics of objects within a dark matter halo is a function of the mass alone. The second is that the clustering of dark matter halos is a function of mass. However, it can be shown that the clustering of halos at fixed halo mass is dependent on the formation time of the halo (Wechsler et al. 2002; Sheth & Tormen 2004; Gao et al. 2005; Wechsler et al. 2006; Croton et al. 2007; Zentner 2007). Furthermore, it has been shown that the clustering of a given halo is dependent on halo concentration (Wechsler et al. 2002, 2006). **[ARZ: Using this twice! argh! Such a sentence is very awkward and unclear. Generally, avoiding using "this" or "that" frequently unless it is absolutely obvious what "this" and "that" are.] [ASV: Hopefully this is more clear and has removed using this repeatedly!]** The additional clustering dependences violate assumptions in the standard implementations; more complicated methodologies have been made to accomodate this by using merger histories directly from simulation (Dvorkin & Rephaeli 2011) or to adjust for the concentration dependence (Gil-Marín et al. 2011). The relationship that clustering has to the properties of the halo is commonly referred to assembly bias or environmental effects.

In this work, we explore a simpler extension of the model in which the size of halos is redefined. This idea of halo redefinition is motivated by the size of a halo not being a well-motivated property. What is often referred to as the "virial radius" will not contain all gravitational bound dark matter particles in the halo (Kazantzidis et al. 2006). Rather, it is a matter of convention that does not share a common definition across the literature. For example, some studies have chosen to use halo radius defined with respect to the critical mass density of the universe, while many simulation papers choose to use the mean background mass density of the simulation. **[ASV: Is there a citation to be used for this? Or is this considered common knowledge within the field?]** Furthermore, the overdensity often used can typically vary from 178 (from basic spherical collapse) to 200 (a common simulation definition) to 337 ("virial" in ΛCDM). This can lead to a ten to twenty percent difference in the measured halo radius between two measurements. We instead choose to define the halo radius to encompass any nearby environmental effects. These may be due to large-scale structure or driven by baryonic physics. Using a simulated box, we then test how the redefinition of halo size affects the relationship between clustering and halo properties. In the case that halo properties become independent of the clustering, it is possible to utilize standard implementations of the halo model without necessitating more complicated modeling. **[ASV: Perhaps I should specifically list halo merger trees as something to be avoided due to computational cost here to motivate the work?]**

In § 2 of this paper, we discuss the cosmological simulations that we analyze and how halos are identified. In § 3, we consider the properties of interest within our halo simulation and their standard definitions. In § 4, we discuss the statistics that we use to measure assembly bias and the removal of known mass scaling from our halo properties. In § 5, we present our results and consider how the change of halo definition impacts measures of assembly bias. In § 7, we discuss the significance of reducing environmental effects through a redefinition of halo environments and discuss possible applications of our methodology. We also consider the nature of assembly bias as a function of halo definition.

2 SIMULATIONS AND HALO IDENTIFICATION

In order to study the effects of halo redefinition, we use three cosmological N-body simulations of structure formation. The Diemer & Kravtsov (2015) simulations each utilize a Planck best-fit cosmology with $\Omega_{\rm M} = 0.32$, $\Omega_\Lambda = 0.68$, and $h_{\rm o} = 0.67$. We use three simulation boxes with comoving sizes of 125, 250, and 500 h^{-1}Mpc respectively. The particle masses are 1.6×10^8, 1.3×10^9, and 1.0×10^{10} $h^{-1}{\rm M}_\odot$ respectively, implying a total of 1024^3 particles in each simulation. Furthermore, the three simulations have different force softening scales of 2.4, 5.8, and 14 h^{-1}kpc . We refer to each simulation as L0125, L0250, or L0500 for the remainder of the paper. This set of simulations allows us to probe the resolution effects inherent in halo finding (due to the varying resolutions of the simulations) and to probe the mass dependence of halo clustering over a wider range of halo masses than would be possible with only one simulation from the set. In particular, L0125 , with its higher resolution, contains the least massive resolved halos, while L0500 has the most robust statistics for the most massive halos as a result of the larger simulation volume.

[ARZ: The following sentences here seem out of place.] [ASV: Probably was attempting to tie it to the rest of the ROCKSTAR calculation, but I'll shift mention of this specifically to the properties section.]

[ASV: new attempt at a paragraph that should be more structurally sound, I hope. The old version is commented out for comparison.] To identify halos, we use the ROCKSTAR halo finder, which works on the phase space algorithm described in Behroozi, Wechsler & Wu (2013). In short, ROCKSTAR determines the initial groupings using a Friends-of-Friends algorithm in phase space before applying the spherical overdensity halo definition in order to determine halo properties of interest. Unbound particles are

removed prior to the calculation of halo mass and other halo properties. Our method of halo redefinition is to change how halo size is calculated as part of the ROCKSTAR pipeline. A halo is given a radius, r_Δ, determined by

$$\bar{\rho}(r_\Delta) = \Delta\rho_{\rm m}. \quad (1)$$

The mean density within a spherical volume of radius r_Δ is $\bar{\rho}$, Δ is the overdensity parameter, and $\rho_{\rm m}$ is the mean background mass density of the entire simulation. The resulting halo size calculation can have a large variation depending on the definition $\rho_{\rm m}$ and the choice of Δ. The former can often be substituted by the critical background mass density. The number chosen for Δ can vary drastically in the literature from $\Delta = 337$ to $\Delta = 178$. We choose to change the size of a halo by treating the overdensity parameter as a tunable choice, expanding the range from $\Delta = 340$ to $\Delta = 10$. While more drastic than the differences between the commonly made choices, this may allow us to account for environmental effects by subsuming them into a larger halo.

[ARZ: Try this paragraph again. It is rambling. Also it has structural flaws such as referring to Δ before defining Δ.]

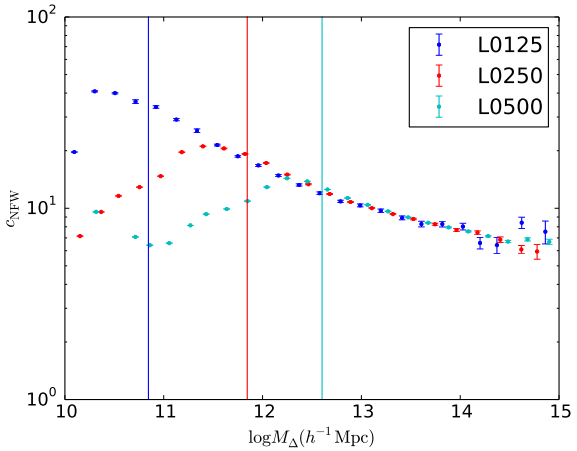

Figure 1. An example of the relationship between the NFW concentration and halo mass for each of our simulations for $\Delta = 200$. The chosen lower limit on halo mass for our sample is marked as a blue, red, or cyan line for L0125, L0250, and L0500 respectively. At lower mass, halos are likely ill defined due to resolution limits.

3 HALO PROPERTIES

We explore the clustering of halos as a function of a number of halo properties that are explored in the literature and can be measured for a halo from an individual simulation snapshot. Halo particles are also fit to a Navarro-Frenk-White (NFW) profile (Navarro et al. 1997),

$$\rho(r) = \frac{\rho_0}{\frac{r}{r_{\rm s}}(1+\frac{r}{r_{\rm s}})^2}, \quad (2)$$

where ρ is the halo density profile and ρ_0 and the scale radius, $r_{\rm s}$, are fit parameters that vary from halo to halo. This allows us to define the halo concentration as

$$c_{\rm NFW} = \frac{r_\Delta}{r_{\rm s}}, \quad (3)$$

where r_Δ is the radius of the halo given an overdensity parameter Δ defining the halo and $r_{\rm s}$ is the halo scale radius. **[ARZ: The scale radius has not yet been defined. How will the reader know what it is? How is it computed? You should probable introduce the NFW profile here rather than above (see my earlier comment on that).][ASV: Should be fixed, although I am a little uncertain as to the introduction of the NFW Profile.]**

We also use an additional measure of the concentration of the halo density profile,

$$c_{\rm V} = \frac{V_{\rm max}}{V_\Delta}, \quad (4)$$

where $V_{\rm max}$ is the maximum circular velocity achieved within the halo and V_Δ is the circular velocity at the halo radius, r_Δ. The quantity $c_{\rm V}$ can be measured from simulations without any need for fitting halo density profiles to determine scale radii and is therefore robust to choices of halo profiles and fitting methods.

Halo concentrations are useful to explore for these purposes for a number of reasons. First of all, environment dependence of concentrations is of direct interest in modeling galaxy clustering and gravitational lensing statistics. Secondly, concentrations can be measured from individual simulation snapshots relatively easily yet halo concentrations are known to be strongly correlated with the formation histories of dark matter halos with earlier forming halos having higher concentrations at fixed halo mass (Wechsler et al. 2002, 2006) **[ARZ: Cite papers here like Wechsler et al. 2002]**. As such, exploring the concentration dependence of halo clustering may yield insight into the age dependence of halo clustering without the need for constructing merger trees. This is particularly important in the present study in which the halo finding is performed repeatedly and constructing a merger tree for each run of the halo finder with different Δ can be prohibitive. We will explore measures of halo age directly in a forthcoming follow-up study dedicated to halo formation histories.

Figure 1 shows the mean $c_{\rm NFW}$-M_Δ relation for halos defined with $\Delta = 200$ in L0125, L0250, and L0500. For each simulation, we consider halos only above a minimum mass, as shown in Fig. 1, to ensure that concentration measurements are not compromised by resolution. Likewise, Figure 2 shows the analogous relation for the alternative definition of halo concentration, $c_{\rm V}$.

Figure 3 shows the relationship between $c_{\rm NFW}$ and $c_{\rm V}$ for quantifying halo concentration on a halo-by-halo basis. Generally the two proxies for concentration are related to each other in a simple manner with relatively small scatter indicating that these two quantities largely contain the same information about each halo.

In addition to halo concentrations, we explore halo clustering as a function of a variety of other halo properties. We explore halo clustering as a function of halo shape quantified by the ratio of the minor and major

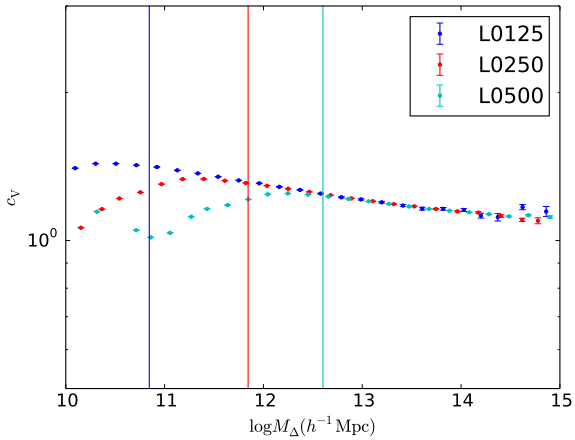

Figure 2. An example of the relationship between the velocity ratio concentration and halo mass for each of our simulations for $\Delta = 200$. The chosen lower limit on halo mass for our sample is marked as a blue, red, or cyan line for L0125, L0250, and L0500 respectively. At lower mass, halos are likely ill defined due to resolution limits.

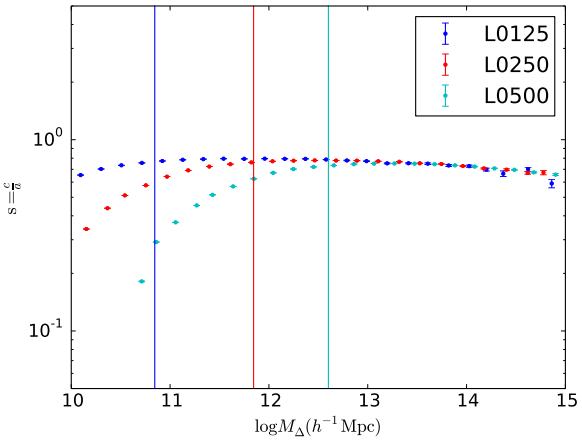

Figure 4. An example of the relationship between halo shape and halo mass for each of our simulations for $\Delta = 200$. The chosen lower limit on halo mass for our sample is marked as a blue, red, or cyan line for L0125, L0250, and L0500 respectively. At lower mass, halos are likely ill defined due to resolution limits.

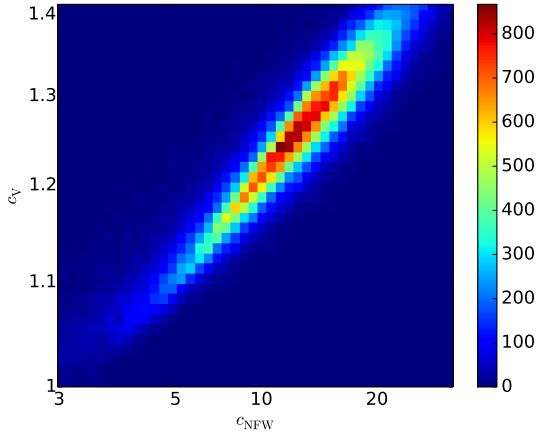

Figure 3. The relationship between the two different marks of concentration, using halos in L0250. The color scale demonstrates the number of halos within a single binning in the concentration space, where redder colors demonstrate where the bulk of halos lie on this relation. **[ARZ: This is not sufficiently specific as a caption. For example, you don't say what the color code is or what the color scale is.][ASV: Hopefully that is sufficient! I'll look into making a label for the color bar though as well, so that it is visible by eye.]**

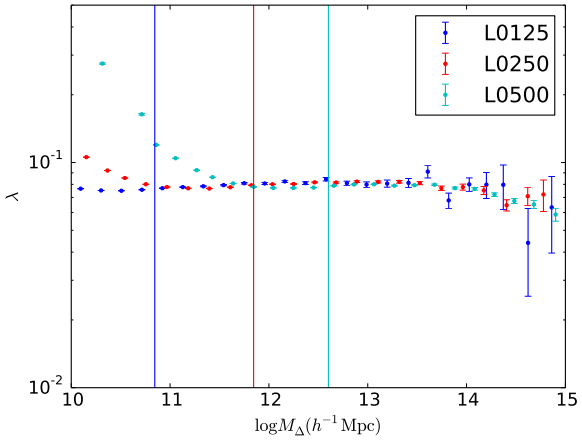

Figure 5. An example of the relationship between halo spin λ and halo mass for each of our simulations for $\Delta = 200$. The chosen lower limit on halo mass for our sample is marked as a blue, red, or cyan line for L0125, L0250, and L0500 respectively. At lower mass, halos are likely ill defined due to resolution limits.

axes length,

$$s = \frac{c}{a}, \tag{5}$$

where a is the major axis length and c is the minor axis length. The mean relations of halo shapes as a function of halo mass for $\Delta = 200$ is shown in Figure 4 along with the mass thresholds selected to ensure that our results are not compromised by resolution.

We also explore halo clustering as a function of halo spin quantified by the spin parameter λ as introduced by (Peebles 1969),

$$\lambda = \frac{J\sqrt{|E|}}{GM_\Delta^{2.5}} \tag{6}$$

where J is the halo angular momentum, E is the total energy of the halo, and M_Δ is the mass at the halo radius, r_Δ. The mean relations of halo spins as a function of halo mas for $\Delta = 200$ is shown in Figure 5 along with the mass thresholds selected to ensure that our results are not compromised by resolution.

In practice, the mean relations between the various halo properties and the mass thresholds must be deter-

mined for each combination of simulation, halo property (e.g., $c_{\rm NFW}$ or s), and halo definition (e.g., value of Δ). We use thresholds determined by the particular case under consideration so as to ensure that resolution limitations do not drive any of our primary results. A higher mass threshold means that we do not have any issues due to halo resolution, but of course, higher mass thresholds reduce statistical power. As an example, we summarize the mass thresholds we have used for a subset of Δ values in Table 1. At most values of Δ, the minimum mass thresholds are driven by the requirement that the halo properties do not suffer significantly from finite resolution effects; if too many low mass halos are included, the true relations can be lost in halos which have insufficient numbers of particles for robust statistics on an individual property. **[ARZ: Please check the veracity of this last sentence. Some such sentence summarizing the factors that limit our mass cuts should be in the paper.][ASV: Slightly modifying this statement due to the fact that I think that multiple parameters are brushed up against the lower limits of the mass cuts.]**

[ARZ: In the table, don't "low mass," "mid mass," and "high mass" correspond to the different simulations? For example, low mass corresponds to L0125 and so on? If not, then I don't understand. If so, then you should label each cut by the relevant simulation name as well.] [ASV: We use the various mass cuts across simulations, so I was going for a more general name - e.g. we use high mass on both L0250 and L0500, which allows us to probe if the relation is driven by the simulation size or the actual mass threshold. I can swap out to more specific names though, but I thought that might cause confusion.]

[ARZ: I would like to see another figure here. I would like to see M_{200} on the x-axis and M_Δ on the y-axis. What should be plotted is the mean M_δ as a function of M_{200} for all halos common to both catalogs. This will be a nice informative plot for the reader and will help the reader to digest the table.] [ASV: Will do using the halo matched catalogs - in progress.]

4 HALO CLUSTERING AS A FUNCTION OF AUXILIARY HALO PROPERTIES

[ARZ: I actually don't understand what you are saying in this paragraph. I hope there is nothing special about L0250 ? Aren't the mass limits determined as you stated in the previous section for each simulation and for each Δ? If so, why does this all need to be repeated here? Perhaps you can just get rid of this paragraph if you are giving this information in the previous section. That would be my preference for logical flow.] [ASV: Agreed. I think this is probably a repeat at this point. There is nothing special about any given simulation.]

4.1 Auxiliary Halo Properties

[ARZ: I thought that the Duffy et al. paper only looked at concentration? Is this correct? Either way, there is an Allgood et al. paper that comprehensively examines this for various halo properties and should be cited here.] [ASV: Found an Allgood paper that is looking at shape, but I'll do a lit search to see if I can't find something else explicit about some of the other parameters] Another well known effect is the scaling of our properties as a function of halo mass, as well demonstrated within the literature (Allgood et al. 2006; Duffy et al. 2008). We are interested in studying the clustering behavior of halos as a function of properties other than mass. As mass is the dominant halo property correlated with halo clustering strength and environment, we refer to the additional properties that we study as "auxiliary halo properties" (those properties other than mass, such as concentration $c_{\rm NFW}$ or shape s).

Most contemporary cosmological N-body simulations, including the set that we study here, do not have a sufficiently large number of halos to make isolating halos of fixed mass, and then further splitting these halos by an auxiliary property, a powerful method with which to study the dependence of clustering on auxiliary properties. Consequently, we study this phenomenon using halo samples selected according to minimum mass thresholds. To do so, we remove the mass dependence of the auxiliary properties as follows.

We take all host halos of interest and sort them by their halo mass, M_Δ. Ten equally spaced bins of log mass are generated to sort these halos into, ensuring that no bin has one or zero halos. The mean value of each halo property is calculated within each bin, and subtracted from the recorded value for each halo in the bin. This removes the strong mass trend in each of these properties, allowing us to avoid a need to just look at halos at some fixed mass. We use these mass-dependence removed concentrations, shapes, and spins in all calculations throughout the paper. **[ASV: More detail is given. I'm not necessarily comfortable with the current ten bin situation and could conceivably switch back to equally populated bins, which allows for more total bins with halos to look at, but unevenly spaced in log mass.] [ARZ: First, you need some equations here. It is unclear to the reader what the word "normalize" means in this context. YOU MUST provide enough information so that someone with access to these simulations could reproduce your calculations. Also, you don't give important details. How many are in the "equal populations" for example. You may also want to add an additional paragraph speculating briefly on other ways to remove the gross mass dependence. You must also say explicitly that we use the mass-dependence-removed concentrations, shapes, and spins in all following calculations. This might not be the exact wording you want to use, but you can decide what you want to call these things.]**

[ARZ: Flesh this out a bit. See the discus-

Table 1. Minimum mass thresholds for each of our analyses depending upon the value of the overdensity, Δ, used to define the halos. In the columns below the values of Δ we show the minimum host halo masses considered in units of $h^{-1}\mathrm{M}_{\odot}$.

Cutoff Name	$\Delta = 200$	$\Delta = 100$	$\Delta = 75$	$\Delta = 50$
low mass	7×10^{10}	8×10^{10}	9×10^{10}	1×10^{11}
mid mass	7×10^{11}	8×10^{11}	9×10^{11}	1.5×10^{12}
high mass	4×10^{12}	5×10^{12}	6×10^{12}	7×10^{12}

sion in Wechsler et al. 06 as a model. The specific values of the thresholds need to be given] [ASV: Slight change - following Wechsler et al 06 does not ever put a specific limit on subhalo velocity and instead places a limit on the ratio between the subhalo velocity and the host velocity as the prime limit. Just making sure that lines up well.]

To mitigate the correlation between halo mass and satellite number, we follow the prescription of Wechsler et al. (2006). We select only host halos with $v_{\rm max,host} \geq 190$ km s^{-1} in addition to the previous mass cuts. This ensures that the satellite counts will be minimally affected by finite resolution. We then select subhalos from the sample based on the criteria that the ratio $v_{\rm max,sub}/v_{\rm max,host} \geq 0.3$. The subhalo velocity function is a very nearly self-similar function (Zentner et al. 2005) **[ARZ: Cite Zentner, Berlind et al. 2005 and references therein on this point.]**, so that scaling subhalo $v_{\rm max,sub}$ by host $v_{\rm max,host}$ in this way eliminates the gross mass dependence of satellite number. The value chosen for this ratio has been adopted such that all host halos that make the above cut contain, on average, one selected satellite halo. As a final selection cut, for each host halo, only the number of subhalos within the radius R_{Δ} of the host are counted.

[ARZ: In the earlier draft, the preceding paragraph had a logical flow that made it very difficult to follow the steps in the calculation. If you think about it for a minute, the important pieces are: (1) we quantify subhalo size with $v_{\rm max,sub}$ because it is more robustly measured than subhalo mass; (2) there is a minimum $v_{\rm max,sub}$ that we can aspire to reach because of resolution; (3) we quantify subhalo number by scaling subhalo size relative to host size, $v_{\rm max,sub}/v_{\rm max,host}$, because this scales out the gross dependence of subhalo number count on host halo size; (4) we must choose host halos that are sufficiently large that the contain, on average, a few subhalos above our minimum subhalo $v_{\rm max,sub}$. These considerations completely specify the cuts on $v_{\rm max,sub}$ and $v_{\rm max,host}$. Please make sure these elements of the logic are clear to the reader.] [ASV: I think the steps should be clear at this point? Let me know if not.]

4.2 Clustering Statistics

We assess the influence of assembly bias on two-point statistics of host halos. In order to do so, we study both the standard two-point correlation functions of halos selected by properties other than mass (e.g., the auxiliary properties concentration, shape, and spin) as well as halo mark correlation functions (MCFs). MCFs quantify the manner in which a halo property (the "mark") correlates among halo pairs as a function of the distance between the pairs. Absent halo assembly bias, halo marks are uncorrelated among pairs. MCFs have been used in several previous papers to quantify environmental dependence of halo properties other than mass (Sheth & Tormen 2004; Harker et al. 2006; Wechsler et al. 2006) **[ARZ: I think there are also a couple of Sheth papers that should be cited here, maybe more]**. For a specific halo property, or mark m, we use the MCF normalization of Wechsler et al. (2006), namely

$$\mathcal{M}_m(r) \equiv (\langle m_1 m_2 \rangle_p(r) - \langle m \rangle^2 / \mathcal{V}(m), \qquad (7)$$

where $m_{\rm i}$ is the value of the mark for halo i, $\langle m \rangle$ is the mean of the mark, and $\mathcal{V}(m)$ the variance of the mark. The notation is intended to indicate that the average is taken over all pairs of halos separated by a distance r. In the absence of any correlation between a halo property and the halo having a neighbor a distance r away, $\mathcal{M}_m(r) = 0$. Deviations of the MCF from zero indicate such correlations exist and the size of the $\mathcal{M}_m(r)$ gives the excess of the mark among pairs compared to the one-point mean of the mark $\langle m \rangle$ in units of the one-point variance.

It is necessary to assess statistical fluctuations in the statistics that we measure in these simulations in order to determine the significance of the signals. For two-point correlation functions, we determine the covariance of the measurement through jackknife resampling of the eight octants of the simulation cube. We assess the statistical significance of the MCFs by randomly re-assigning each of our marks to the halos in the sample. We then compute the MCF of these randomized marks. As the mark re-assignment is random, the MCF computed on these re-assigned marks *cannot* exhibit any environment dependence other than that induced by statistical fluctuations. We perform this reassignment 400 times and approximate a 2σ error region by the span of the MCF between our $10^{\rm th}$ lowest and $10^{\rm th}$ highest (that is the $390^{\rm th}$ if the MCFs were sorted in ascending order) values of the MCF. In the event that there are no environmental correlations with halo auxiliary properties, the MCFs measured in the simulations would fall within this error band 95% of the time.

[ARZ: The sentences immediately below this comment can be removed. Also, not a wise idea to lock yourself into 20% in the text. There is absolutely nothing special about 20%. In fact, it would be interesting to see if things change as this percentile changes, perhaps try 50% and 10%. We should at least know what those figures look like

before proceeding to publication, so you should make them even though we likely won't include them in the main text of the paper. It could be very informative and will almost certainly be useful when giving talks.][ASV: Removed - the new framework with halo tools makes it easier to test any cut that we want in short order as well.]

5 RESULTS

[ARZ: We don't need to reiterate all of this stuff about the mass cuts. Just make sure the discussion in the simulations section is complete and then we can move forward. Again, I suggest changing the names of your cuts. It would be great if they can signify something either about the ACTUAL MASS involved in the cut or the simulation or possibly BOTH! Perhaps you can say the "L0125" cut and so on? If you get everything specified in the simulation section, then this paragraph is completely unnecessary.][ASV: Removed - still debating how to name these cuts.] [ARZ: It seems to me that we DO include L0500 !! Even if we don't we should. Let's treat each simulation as simply sampling a different range of halo masses. That is the most useful way to proceed.][ASV: Also removed - this was leftover from the old plots, before L0500 was included in all the plots.]

5.1 Correlation Functions

[ARZ: Fix up and fill in numbers as needed, but follow this general format.] We begin by studying the correlation functions of halos in our mass threshold samples, sub-selected by auxiliary properties. Figure 6 exhibits the difference between the clustering strength of halos in the $20^{\rm th}$ percentile highest concentrations and the halos with the halos that have the $20^{\rm th}$ percentile lowest concentrations as a function of the overdensity parameter Δ, used to define the halos. First, it is clear that clustering strength generally depends upon the auxiliary properties of halos at all halo mass thresholds. Second, it is clear that the strength and sign of assembly bias is strongly mass dependent, a result that agrees with the significant previous literature on halo assembly bias (Wechsler et al. 2002; Gao et al. 2005; Zentner 2007; Wechsler et al. 2006; Harker et al. 2006; Croton et al. 2007; Dalal et al. 2008)**[ARZ: Cite all the usual papers here, Gao, Wechsler, Harker, Zentner07, Dalal07, probably several more.][ASV: I think that is most of the usual suspects, but I'll do a double check for more important ones!]** At relatively low mass (the L0125 panel, $M_{200} > 7 \times 10^{10}\ h^{-1}{\rm M}_{\odot}$), high-concentration halos are considerably more strongly concentrated than low-concentration halos using the more conventional $\Delta = 200$ definition for halos. At somewhat higher halo masses (the L0250 panel, $M_{200} > 7 \times 10^{11}\ h^{-1}{\rm M}_{\odot}$), this difference is markedly reduced. Finally, for the highest mass halos that we have the capability of studying (the L0500 panel, $M_{200} > 4 \times 10^{12}\ h^{-1}{\rm M}_{\odot}$), the effect is of opposite sign; low-concentration halos are more strongly correlated than high-concentration halos.

[ARZ: The language in this paragraph is way too loose and not sufficiently clear or professional. What does it mean to be a "reasonable" mass range, for example? I'll attemp to clean it up. Try to follow this model in your writing. Compare my version:] Focus first on the middle panel of Fig. 6. In this panel, corresponding to the L0250 mass threshold, the difference in large-scale clustering between high- and low-concentration halos is dramatically reduced for a halo definition with $\Delta = 75$. Further decreasing Δ leads to concentration-dependent clustering of opposite sign. Comparing the differing clustering strengths across the three panels of Fig. 6, it is clear that this is not a universal conclusion. For low-mass halos, very low values of Δ (and correspondingly large definitions of halo radii, as $R_{\Delta} \propto \Delta^{-1/3}$) are necessary in order to mitigate the concentration dependence of halo clustering. Conversely, for higher mass halos (the L0500 panel), values of $\Delta \approx 200$ yield little concentration-dependent clustering. In this case, decreasing Δ (increasing R_{Δ}) results in significantly *increased* concentration-dependent halo clustering. The reasons for these changes is of interest and we return to interpreting these results below.

Notice that in all panels of Fig. 6, the effect of concentration-dependent clustering is scale-dependent. Moreover, the effect is scale-dependent for all values of Δ. In these cases, simply defining halos with a different value of Δ does not suffice to eliminate concentration-dependent clustering on all scales. In this discussion and throughout, we focus primarily on the large scale clustering, which we take to mean clustering on scales significantly larger than the radii, R_{Δ} of the halos in our samples. In each panel in Fig. 6, we designate the radii of the largest halos in each sample with vertical dashed lines.

[ARZ: Given how the correlation functions look, shouldn't we include results for $\Delta < 50$, for the L0125 results? The effect is continuous so it looks like it would be removed with a smaller value of Δ, say $\Delta \approx 20$. I think you have run this already, so no reason to leave it out. I say this is a must for moving forward with publication.] [ASV: Definitely in the works for L0125! Just finishing up some runs in order to sort things out.]

[ARZ: On another note, did you ever compute these things for finer spacing of Δ? For example, it looks like $\Delta \approx 70$ is going to work better than $\Delta = 75$. It's OK if you haven't, but let me know! I thought we had discussed this.] [ASV: We have some finer spacing to investigate from previous runs.]

[ARZ: For the high-mass, L0500, cut, did you try any $\Delta > 200$, maybe $\Delta = 210$ or so? This is not really necessary, I'm just curious how this looks.] [ASV: We also have finished a $\Delta = 340$ run of this to examine as necessary.]

[ARZ: I assume that if you made the same plot for c_V we would reach the same basic conclusions as for c_{NFW}? If this is so, then you need

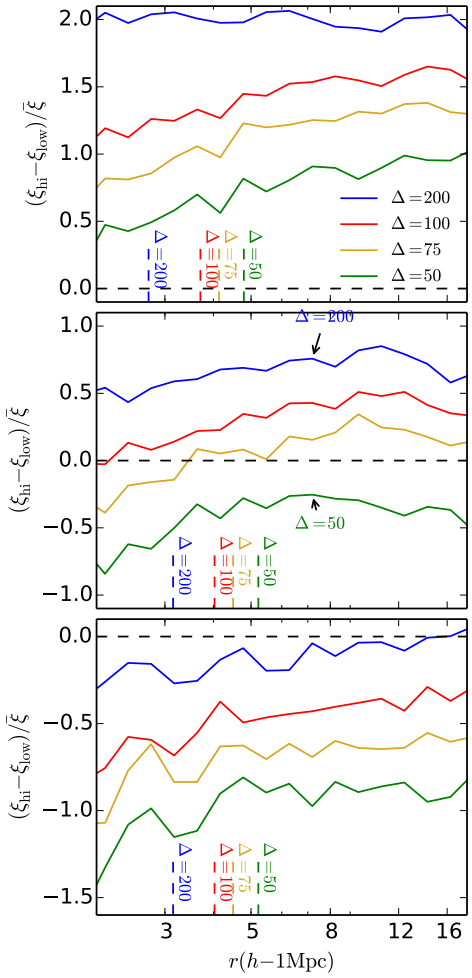

Figure 6. [ARZ: All lines here could stand to be slightly thicker.] The difference of the correlation function for only the top 20% most concentrated halos and the bottom 20% in concentration, normalized by the overall correlation function of the entire sample. From top to bottom we show the results for the lowest mass cut in L0125, L0250, and L0500 that excludes ill resolved halos. [ARZ: This method of specifying the mass cuts is poor style. You already gave each mass cut a name in the table. Why now use a different way of referring to the mass cuts? This confuses the reader, and even I find it confusing. I'm not sure what the plot shows! Just use the names of the cuts!] The dashed lines along the bottom denote the largest halo radius for a given value of the overdensity parameter. [ARZ: This figure needs to be remade. Labels need to be cleaned up. Each panel needs to be labeled with simulation name and mass threshold (as an aside, I prefer the word "threshold" to "cut"). I also think that you could stand to make the figure a little bit bigger. Not a big deal to me. Lastly, this figure doesn't give a good sense of the statistical error. How about putting error bars on one of these lines? Perhaps on the $\Delta = 75$ line in the middle panel. That is the most important one to have error bars on.]

to add a specific statement in this regard to the end of the discussion above. In this case, no new figure would be needed. If not, then you need to show the figure.] [ASV: This information is not currently run, but should be trivial to add to the halotools setup. I'll add it after this initial recheck with the new normalizations.]

[ARZ: In this subsection, I advocate at least one and perhaps two new figures. First, can you make an analogous plot to Fig. 6 that shows some other property, such as shape or spin? This would be a nice addition for completeness. Second, what would happen if you used 50% or 10% cuts on concentration? Would we reach nearly the same conclusions? If so, then you do not need to show the plots explicitly. However, in this case, you DO need to state explicitly that this is the case. In other words, you need to state the the broad conclusions we reach are roughly independent of the specific percentiles that we use to select halos so that showing results for a variety of different percentiles doesn't add very much to the discussion. It is also possible that selecting on a different percentile yields an entirely different conclusion. I don't suspect that this will be the case, but it is possible. If that happens, then you need to show an example of such a figure for, say, concentration.] [ASV: Can definitely do all of this pretty straightforward now. The plotting pipeline is all ready to go and the halo concentration cuts are fairly minimal in terms of time constraints compared to the rest of the global work. I'll do cuts for all properties at 10%, 20%, and 50% for purposes of testing, especially given our concern for the tails.]

5.2 Mark Correlation Functions

We now move toward a discussion of halo assembly bias as diagnosed by MCFs. MCFs have the advantage that it is not necessary to specify particular auxiliary property subsamples, such as the percentiles above, in order to assess assembly bias[1] The NFW concentration, $c_{\rm NFW}$, MCF is shown in Figure 7. The shaded bands in the figure delineate the statistical fluctuations in MCFs induced by finite sampling as discussed in the previous section. Qualitatively, Fig. 7 exhibits the same features that are evident in Fig. 6: more concentrated halos are significantly more clustered in the low-mass L0125 halo sample; concentration-dependent halo clustering weakens and reverses sense as halo mass increases; for the L0250 sample with $\Delta = 70$, the large-scale concentration dependence of halo clustering has been reduced so as to be

[1] Of course, this comes at the cost of averaging over all values of the auxiliary properties. Using MCFs it is not evident if the assembly bias effect is a smooth function of the auxiliary properties, dominated by the tails of the auxiliary property, or has some more complex dependence upon the auxiliary property. Our results in § 5.1 suggest that assembly bias is a fairly smooth function of the auxiliary properties.

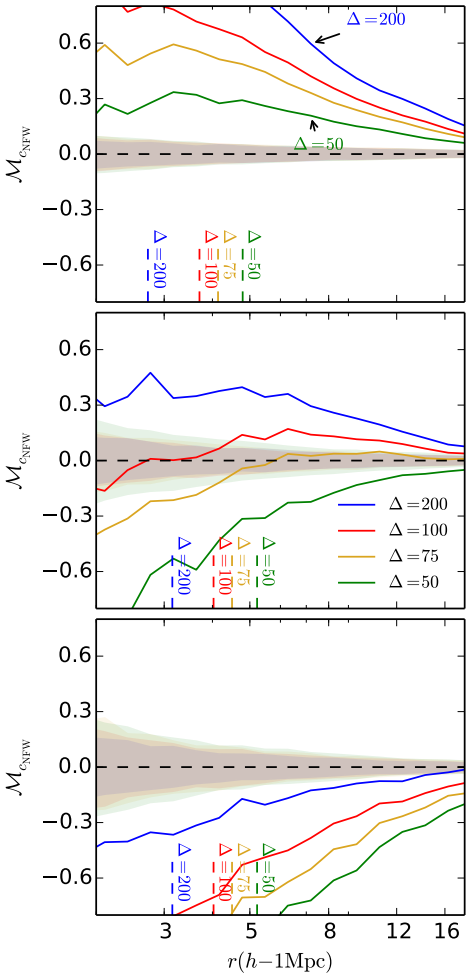

Figure 7. **[ARZ: Many of the same comments from the previous figure are also relevant here, label mass cuts/simulations in each panel etc.]** The marked correlation function for the concentration defined according to the NFW profile. From top to bottom we show the results for the lowest mass cut in L0125, L0250, and L0500 that excludes ill resolved halos. The shaded bands represent 2-sigma confidence regions generated by randomization of the marks. The dashed lines along the bottom denote the largest halo radius for a given value of the overdensity parameter.

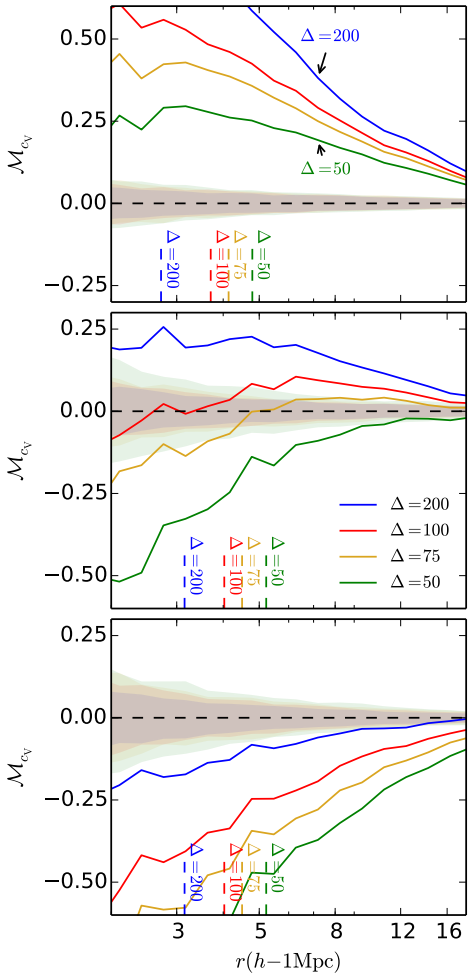

Figure 8. The marked correlation function for the concentration defined according to the velocity ratio. From top to bottom we show the results for the lowest mass cut in L0125, L0250, and L0500 that excludes ill resolved halos. The shaded bands represent 2-sigma confidence regions generated by randomization of the marks. The dashed lines along the bottom denote the largest halo radius for a given value of the overdensity parameter. **[ARZ: Bottom panel here needs to be fixed so lines don't run into labels and virial radii markers and so on. Label each panel by simulation and/or mass cut for M_{200}.]**

consistent with zero within the statistical limitations of the simulation. **[ARZ: Again, it seems like we need a $\Delta < 50$ line for L0125. If possible, it would be great if we could put a $\Delta > 200$ line on this plot for the L0500 simulation.]**

Figure 8 is a similar plot for the velocity-defined concentration, $c_{\rm V}$ MCF. This figure exhibits qualitatively and quantitatively similar features to Fig. 7, a fact that is not surprising given that we already know that $c_{\rm NFW}$ and $c_{\rm V}$ quantify largely redundant information about their halos.

Moving on from concentrations, Figure 9 illustrates MCFs in which the mark is the shape parameter, s, of the halo. The environmental dependence of shape parameter is distinct from that of concentration in a number of ways. Notice that at all masses and at all halo definitions, less spherical halos (halos with smaller s) are more strongly clustered. Furthermore, decreasing Δ (increasing halo radius) only serves to increase this environmental dependence in all cases. This is indicative of halo shapes being driven by structure on scales larger than halo radii, in particular R_{200}, and is not entirely surprising given our significant amount of knowledge of the filamentary nature of large-scale structure. **[ARZ: If possible, a line here with $\Delta \gg 200$. Seems like it could be instructive, let me know if this is going to take a long time or be very onerous.]**

The spin MCFs are shown in Figure 10. Qualitatively, spin-dependent halo clustering is quite similar

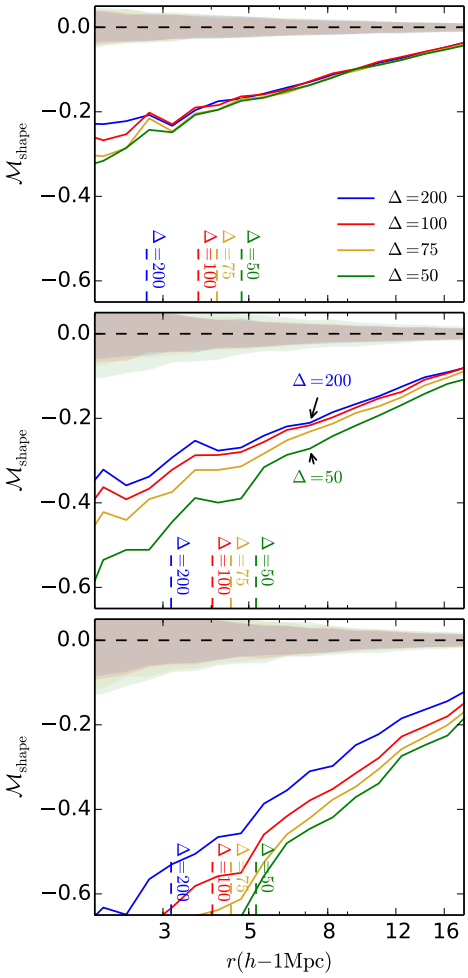

Figure 9. The marked correlation function for the shape of the halo. From top to bottom we show the results for the lowest mass cut in L0125, L0250, and L0500 that excludes ill resolved halos. The shaded bands represent 2-sigma confidence regions generated by randomization of the marks. The dashed lines along the bottom denote the largest halo radius for a given value of the overdensity parameter. **[ARZ: Bottom panel here needs to be fixed so lines don't run into labels and virial radii markers and so on. Label each panel by simulation and/or mass cut for M_{200}.]**

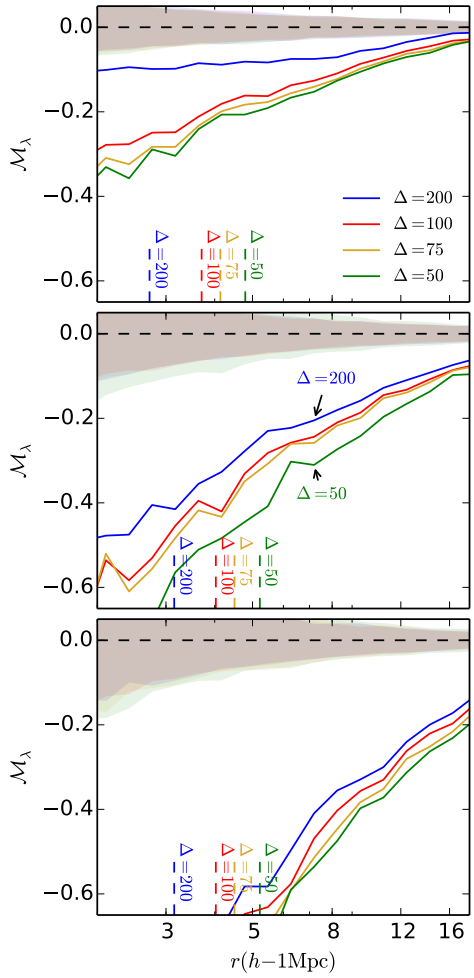

Figure 10. The marked correlation function for the spin parameter of the halo. From top to bottom we show the results for the lowest mass cut in L0125, L0250, and L0500 that excludes ill resolved halos. The shaded bands represent 2-sigma confidence regions generated by randomization of the marks. The dashed lines along the bottom denote the largest halo radius for a given value of the overdensity parameter. **[ARZ: Bottom panel here needs to be fixed so lines don't run into labels and virial radii markers and so on. Label each panel by simulation and/or mass cut for M_{200}.]**

to shape-dependent halo clustering. Halos of low-spin cluster more strongly than halos of high-spin. **[ARZ: Search the literature, particularly Brandon Allgood's papers and Andreas Faltenbacher whose names come to mind, for spin-dependent assembly bias. I'm trying to figure out if yours is the first paper to point this out.]** Likewise, increasing halo radii by decreasing Δ in halo definitions only drives spin-dependent halo clustering to be stronger.

The clustering of halos as a function of the number of satellite galaxies at fixed mass is of particular practical interest. Efforts to model survey data on the large-scale galaxy distribution, such as the halo occupation distribution (HOD) or conditional luminosity function (CLF) formalisms typically make the assumption that the multiplicity of satellite galaxies within a host dark matter halo depends solely upon halo mass. If this assumption is violated, then the phenomenological modeling of galaxy clustering can be more complicated than in these simplest scenarios.

Figure 11 shows clustering marked by satellite number as described in § 4. For all values of Δ, halo clustering is strongly dependent upon satellite occupation at all masses. Interestingly, altering halo definitions as we have makes little difference to this dependence. In fact, defining halos to have larger radii (smaller Δ) generally makes the environmental dependence of halo clustering more significant. Of course, our results pertain to satellite halos, or subhalos, rather than satellite galaxies, so

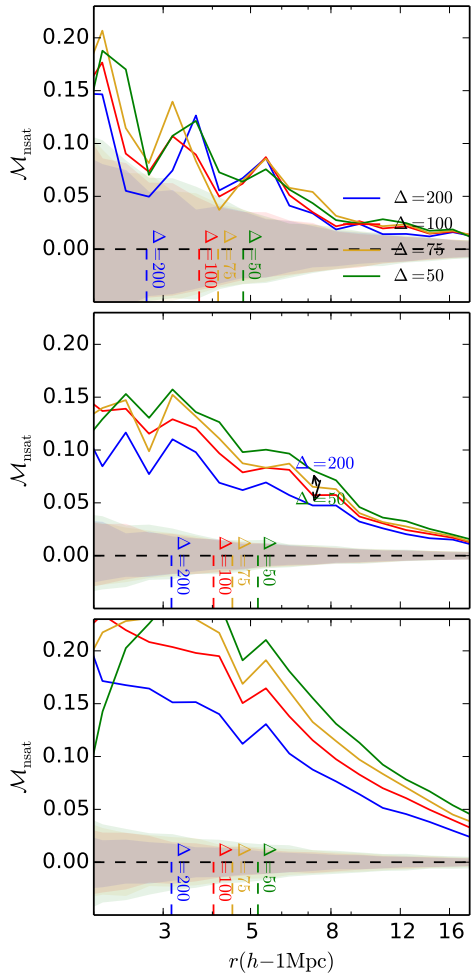

Figure 11. The marked correlation function for the number of satellites for a host halo. From top to bottom we show the results for the lowest mass cut in L0125, L0250, and L0500 that excludes ill resolved halos. The shaded bands represent 2-sigma confidence regions generated by randomization of the marks. The dashed lines along the bottom denote the largest halo radius for a given value of the overdensity parameter. **[ARZ: Many obvious cosmetic problems with this figure that need to be fixed.]**

the connection to observations and how one might model observed galaxy clustering is indirect, yet suggestive.

6 DISCUSSION

[ARZ: Repeating this comment here because of its importance. Look in the literature to see if spin-dependent halo clustering has been measured in the literature before. Look at http://arxiv.org/abs/1207.4476.]

We have shown (confirmed or reiterated may be a better word here) that for conventional halo definitions halo clustering strength is a strong function of "auxiliary properties" halo concentration (either measured through a fit to the NFW profile or assigned non-parametrically as the ratio of the maximum circular velocity to the virial velocity), halo shape, halo spin, and number of subhalos for host halos over a wide range of masses. These findings are consistent with the now significant literature on the subject subject of halo assembly bias **[ARZ: Reiterate citations here.]**

We have explored the efficacy of alternative halo definitions to mitigate the dependence of halo clustering on these "auxiliary properties." Rather generally, we find that these alternative definitions do *not* mitigate the effects of assembly bias. In most cases, defining halos to have significantly larger radii (lower Δ) than in conventional halo definitions had only a modest influence on these assembly bias effects. Moreover, to the degree that these modified halo definitions had any effect at all, it was often of the sense of making the assembly bias effect stronger, rather than weaker.

One exception to this general conclusion is the case of halo concentration. Our results suggest that halo redefinition may be able to mitigate concentration dependent halo clustering. This is evident in Fig. 7 and Fig. 8. Halo concentration is strongly correlated with halo formation time, so this suggests that such a redefinition may also aid in reducing assembly bias associated with halo formation time; however, this is a non-trivial extrapolation of our results and a follow-up study to assess halo formation times in alternative halo definitions is both interesting and warranted.

Clearly, the halo definition that best mitigates concentration-dependent assembly bias must be mass dependent. Low values of Δ ($\Delta \sim 25$ with $R_{25} \sim 2R_{200}$) seem appropriate near for our lowest mass-threshold sample (with $M_{200} \geq XXX$) whereas $\Delta \sim 200$ or slightly higher is adequate for our highest mass threshold sample (with $M_{200} \geq YYYY$). This result is reminiscent of much recent work on the so-called halo "splashback radius." **[ARZ: Here, compare our results to the splashback radius work.]**

[ARZ: Here is where we could use ANOTHER FIGURE! What I would like to see is a visual comparison of our "best" Δ as a function of halo mass threshold compared to the equivalent for the splashback radius. To be clear, it is trivial to go back and forth between Δ and radius (since radius $\propto \Delta^{-1/3}$) so this can be represented with either Δ or radius. If you choose to use radius, then it should probably be normalized, such as R_Δ/R_{200} and $R_{\rm splashback}/R_{200}$ and so on. This could be an important figure and point to future work on this subject.]

It is useful to investigate the reasons why halo redefinitions may be helpful in the case of concentrations. On the positive side, it is possible that these redefinitions do define halos an a more practically useful way, better isolating objects that have been strongly altered by nonlinear evolution from the larger-scale environment. In this case, halo redefinition would be a step forward. However, it is also possible that the details of measuring halo properties using these new halo definitions introduce new sources of noise into the measurements. If this is the case, then the reduction in environmental effects stems from the fact that them measurement of the halo property in-

troduces noise and is *less* informative about the halo itself. For the case of halo concentration, which is the most interesting to follow up, introducing noise can happen in numerous ways. For example, the NFW concentration $c_{\rm NFW}$ is determined by a fit to the NFW profile. Inferred values of $c_{\rm NFW}$ will depend upon the degree to which the density profiles of the halos follow the NFW functional form within some radius R_Δ that is different from traditional halo radii, such as $\sim R_{200}$. At large halocentric distances ($r \gtrsim R_{200}$) halo profiles are known to deviate from the NFW form. It is worth noting that the velocity-defined concentration $c_{\rm V}$ is a non-parametric measure of concentration and should be less subject to such effects.

[ARZ: New figure needed here. This should be, for the L0250 simulation (my guess this one is most instructive, but use your judgment here), a comparison of the concentration-mass relation for halos defined with $\Delta = 200$ to the concentration-mass relation for halos defined with $\Delta = 70$ (of whatever you deem best). The figure must represent both the mean (or median) relation AS WELL AS the dispersion in this relation at fixed mass. The plot should exhibit this for both $c_{\rm NFW}$ and $c_{\rm V}$. Two panels may be necessary to make these points.]

As such, it is useful to examine the concentration-mass relations for halos in the simulations for various halo definitions. This is shown in **[ARZ: NEW FIGURE.]** Notice that **[ARZ: Now you mention the interesting part about the new figure. This should be a discussion of how much larger/smaller the dispersion in concentrations gets for, say $\Delta = 70$ compared to $\Delta = 200$.]**

We can explore in more detail the degree to which the mitigation of environmental effects by halo redefinition are due to introducing noise that is uncorrelated with environment into the measurement of halo properties when halos are defined in a manner distinct from the more traditional definitions. We proceed as follows. All host halos that are found in the halo catalogs constructed from lower values of Δ (for example, Δ 70 which is an interesting value for exploring concentration in the L0250 simulation) are present as host halos in the halo catalogs constructed with higher values of threshold density (e.g., $\Delta = 200$). We match each halo in the lower threshold (lower Δ) simulation to its corresponding halo in the higher threshold catalog. We then consider the clustering of only those halos that we have matched across catalogs. We refer to these as the "matched" halo samples between two values of threshold overdensity Δ.

[ARZ: I removed the correlation function comparison here. It is too busy to read and not necessary. It also opens up the whole Pandora's box of "why choose 20%?" I'd rather avoid that in this discussion. Let's just jump straight to the MCF. This will reduce the proliferation of figures as well.]

[ARZ: Please check to ensure that I know what you mean by your matched samples. Your language was not specific enough for me to be 100% sure. Modify as necessary.] Figure 12 shows a comparison between the standard $\Delta = 200$, $c_{\rm NFW}$ MCF and the MCF of the matched subsamples. The matched subsamples are matched to the $\Delta = 70$ halo catalogs and differ from the standard halo samples in that they contain only those host halos common to both the catalog in question and the $\Delta = 70$ catalog. The most interesting matched sample to examine in this case is the $\Delta = 200$ sample. In this sample, all halos are defined as they would be defined in the $\Delta = 200$ catalog, including all inferred halo properties; however, the matched catalog contains only those host halos that also appear in the $\Delta = 70$ halo catalog. Therefore, many host halos have been removed from the sample because they have become subhalos in the $\Delta = 70$ catalogs.

From Fig. 12, it is apparent that some degree of assembly bias persists in the matched samples. Yet, what is interesting is that a very significant fraction of the assembly bias effect has been removed compared to the standard $\Delta = 200$ result. The halos in the matched catalogs have the same properties (including $c_{\rm NFW}$) as those in the standard catalogs, so that removal of assembly bias is *not* due to introducing noise or other systematics into the measurement of concentration. That mitigation of assembly bias is due to the halo redefinition and, in particular, subsuming those halos most subject to assembly bias effects as subhalos of the $\Delta = 70$ halos. This is an interesting result suggesting that seeking optimal halo definitions may be one avenue to more completely separating the strongly nonlinear evolution occurring within halos from large-scale evolution and mitigating assembly bias.

[ARZ: Put a discussion of Fig. 13 here. It does not need to reiterate the discussion of Fig. 12. However, it should state that we reach the same broad conclusion and that this is good in part because $c_{\rm V}$ is a nonparametric measure of halo concentration.]

[ARZ: Would it be easy for you to plot the concentration-mass relation for only those host halos in the "matched" $\Delta = 200$ sample? If so, that would be potentially interesting for our interpretation.]

[ARZ: We probably don't need the shape, spin, and nsat figures because these don't work anyway! No need to interpret something that is not working.]

[ARZ: Next two paragraphs can be largely removed, starting here ...] However, it is worth noting that statistics such as spin parameter, shape, and satellite numbers do not benefit from this selection effect. Assembly bias in these statistics remains nearly identical, suggesting that the selection effects that preferentially account for backsplash halos do not impact these marks. This does serve as a consistency check: given that our methodology does not seem to have a positive impact on the behavior of these marks, the fact that this selection criteria would have positive impact on the data would be an oddity. Instead, we have another confirmation as to the intrinsic ties between these halo statistics and environment.

Given that the removal of assembly bias is not being driven by introducing noice, we now will attempt to determine why the different marks exhibit different be-

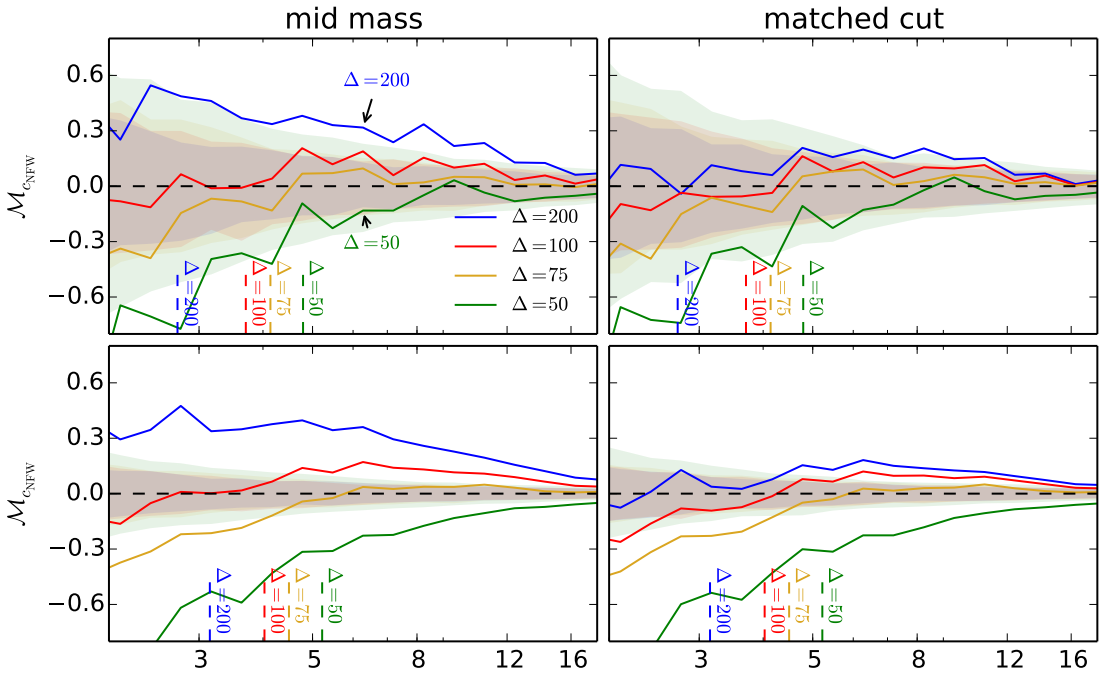

Figure 12. The marked correlation function for the concentration defined according to the NFW profile. The left (right) panel shows the "mid mass" ("matched") cut on L0125 and L0250. The "matched" cut accounts for potential backsplash halos, as discussed further in the text. The dashed lines along the bottom denote the largest halo radius for a given value of the overdensity parameter. **[ARZ: Adopt new labeling scheme. Refer to the simulation, L0250, and the mass threshold rather than using the label "mid mass." Try as best you can to minimize overlaps in the figure. The L0125 is so noisy that it doesn't add anything here, we don't need those panels. I actually don't even think we need more than one panel. The ONLY panel we need is the lower right panel for the L0250 "matched" sample. Add to this panel as a light blue, thick line in the background the standard result for the L0250 box (this standard result is the blue line in the left panel). Then the reader can compare directly the two lines of greatest interest, which are $\Delta = 200$ (no matching) and $\Delta = 200$ "matched." That is all we need unless I misunderstand something.]**

haviors. The first interesting feature is how well our two separate definitions of concentration interact with each other. In the case that the halo can be described well by an NFW profile, one expects a direct relationship between the NFW defined halo concentration and the velocity ratio defined halo concentration. While some variation can be expected due to halos not perfectly being fit by an NFW profile, we do see that the features in one concentration proxy are mirrored in the other. This allows for the two concentration markers to support each other well with regards to our ability to remove environmental effects on large scales. **[ARZ: ... and ending here.]**

[ARZ: This paragraph is good, but needs to be written a bit more professionally. Start with a sentence like, "It is interesting to explore the reasons that halo shape, spin, and satellite number are not amenable to having their assembly bias mitigated through simple halo redefinitions." Then move on to some specifics.] Halo shape and satellite number are statistics that do not end up having their environmental effects removed and can even be made more prominent by our methodology. One intuitive way to consider the former statistic is in the context of the cosmic web. Studies have shown a statistically significant alignment between filaments and satellite galaxy position (Tempel et al. 2015; Velliscig et al. 2015). Our method then expands the halo radius and subsumes material that was previously outside of the halo. A simple graphic illustrates this potential effect in Figure 17. As there is a preferential distribution of these satellites that are being subsumed into the halo, this would serve to induce a shape to the halo that would then be determined by Rockstar. In addition, as our satellite number is chosen by those halos within the halo radius, we anticipate that the most clustered regions would see the largest increase in satellite count and thus see an increase in the satellite number mark.

[ARZ: The way that the paper has been retooled makes this mass cut discussion completely redundant with the main discussion in the paper. The mass dependence is now a fundamental part of the main line of reasoning in the paper and the summary plot I asked for comparing to splashback work will emphasize this point. This can all be eliminated, ... STARTING HERE...] Given the differences between the simulation results and with the data available to us with the Diemer & Kravtsov (2015) simulations, we then explore the effect of the choice in mass cut. The low mass cut effects are shown in the Figure 18 through Figure 23. This cut explores the area in

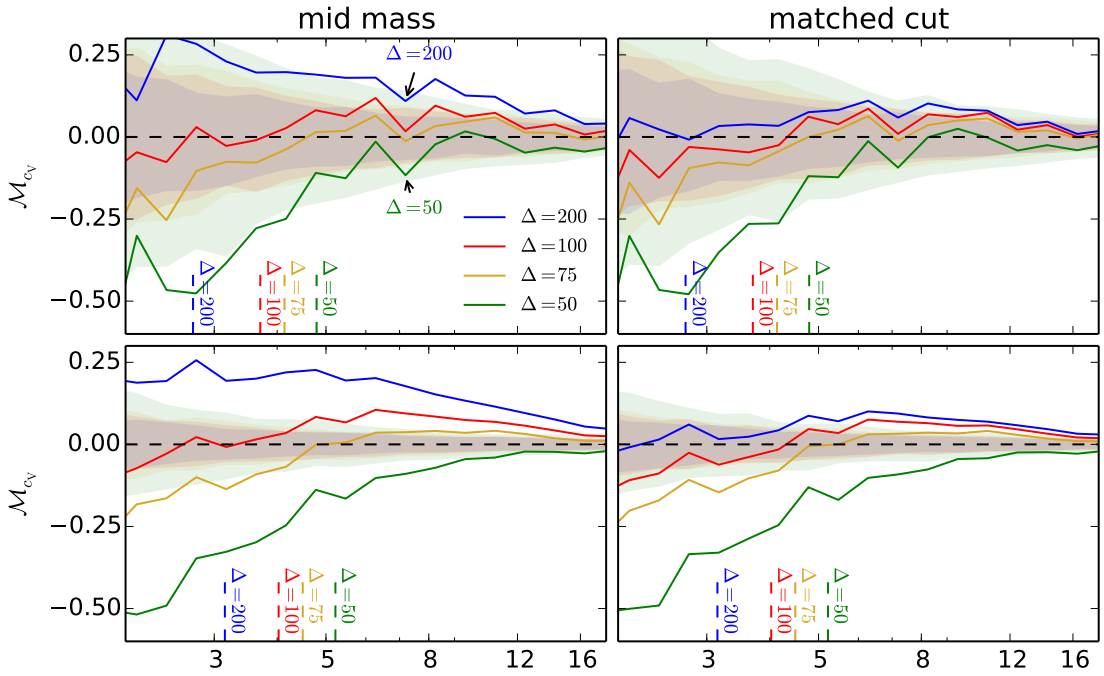

Figure 13. **[ARZ: All the same comments as for the $c_{\rm NFW}$ figure.]** The marked correlation function for the concentration defined according to the velocity ratio. The left (right) panel shows the "mid mass" ("matched") cut on L0125 and L0250. The "matched" cut accounts for potential backsplash halos, as discussed further in the text. The dashed lines along the bottom denote the largest halo radius for a given value of the overdensity parameter.

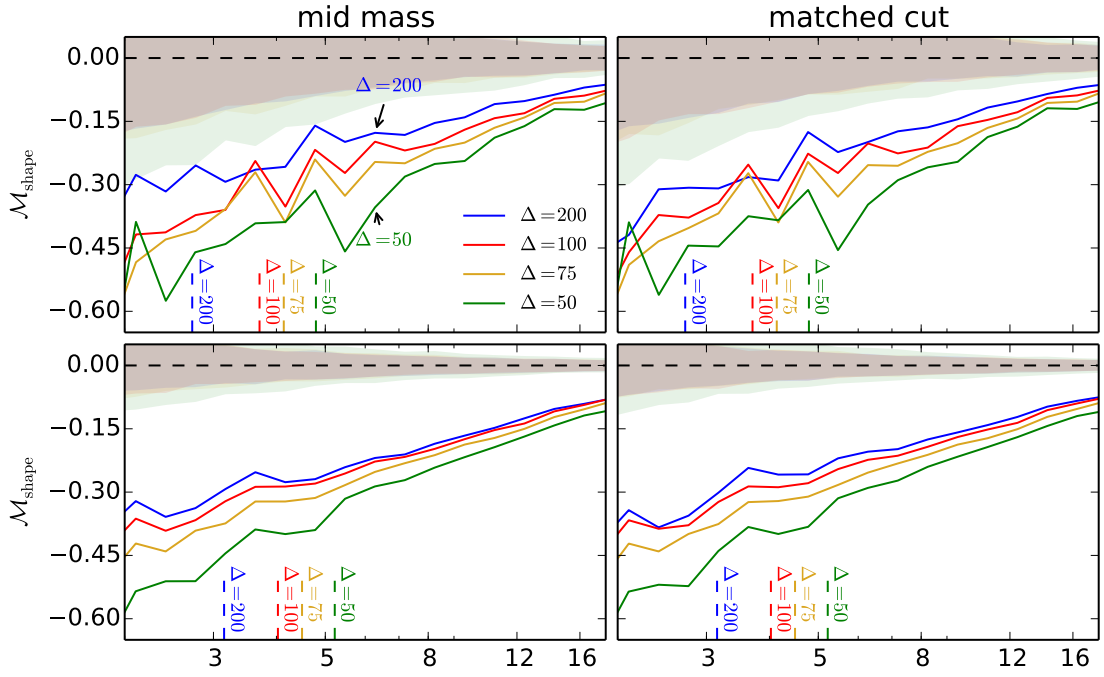

Figure 14. The marked correlation function for the shape parameter. The left (right) panel shows the "mid mass" ("matched") cut on L0125 and L0250. The "matched" cut accounts for potential backsplash halos, as discussed further in the text. The dashed lines along the bottom denote the largest halo radius for a given value of the overdensity parameter.

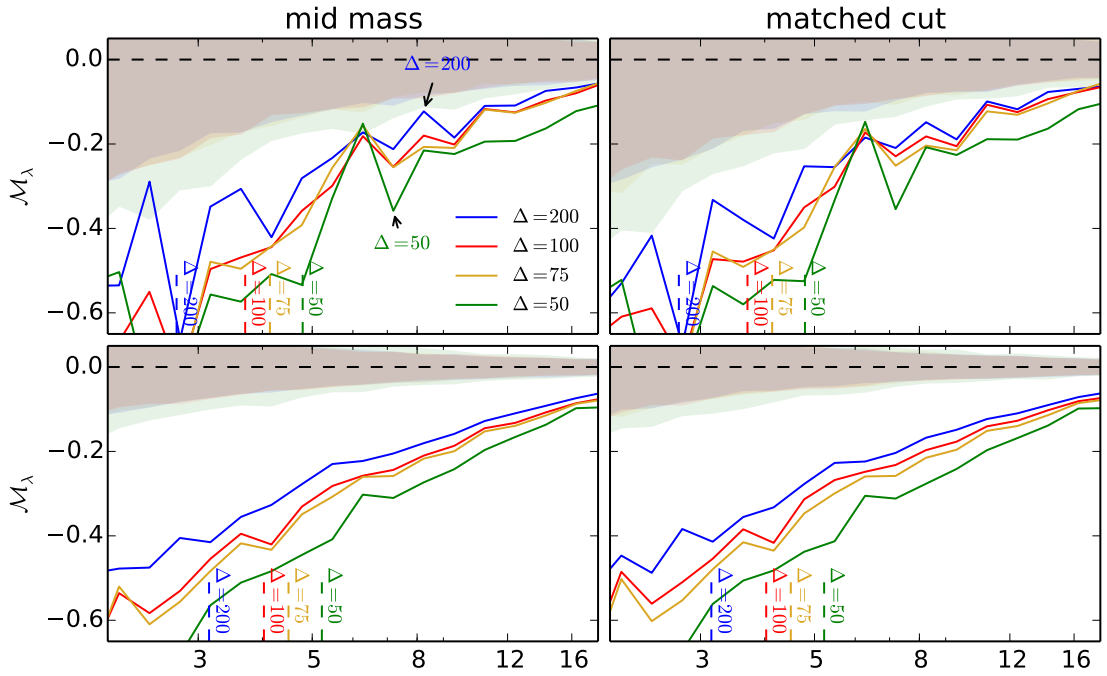

Figure 15. The marked correlation function for the spin parameter. The left (right) panel shows the "mid mass" ("matched") cut on L0125 and L0250. The "matched" cut accounts for potential backsplash halos, as discussed further in the text. The dashed lines along the bottom denote the largest halo radius for a given value of the overdensity parameter.

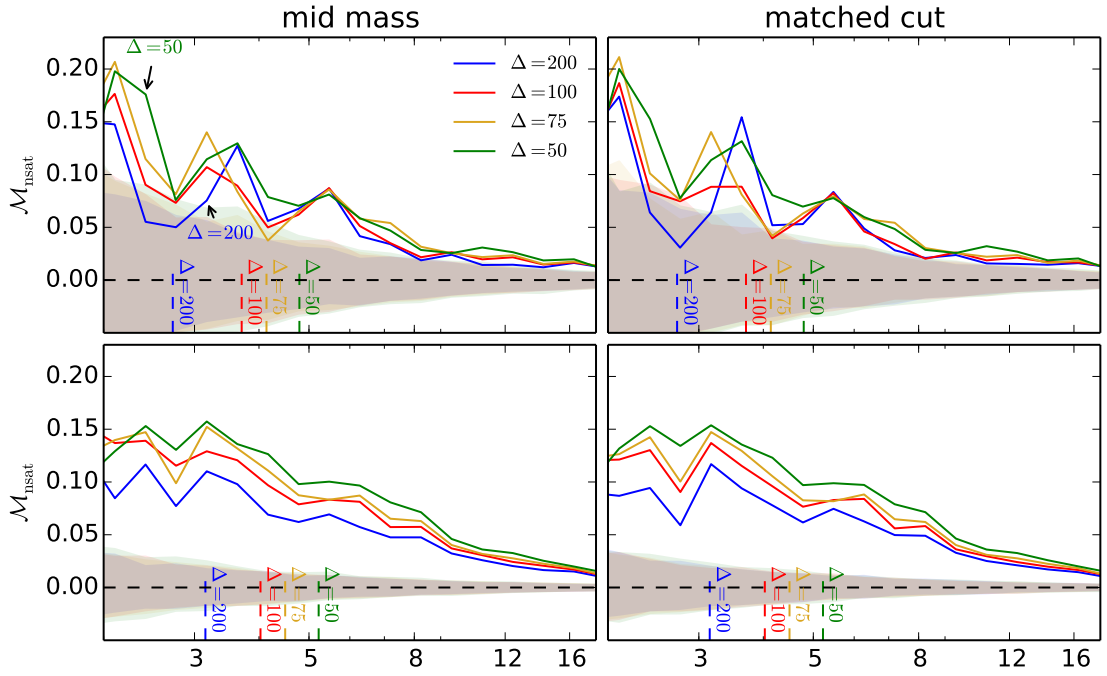

Figure 16. The marked correlation function for the satellite number. The left (right) panel shows the "mid mass" ("matched") cut on L0125 and L0250. The "matched" cut accounts for potential backsplash halos, as discussed further in the text. The dashed lines along the bottom denote the largest halo radius for a given value of the overdensity parameter.

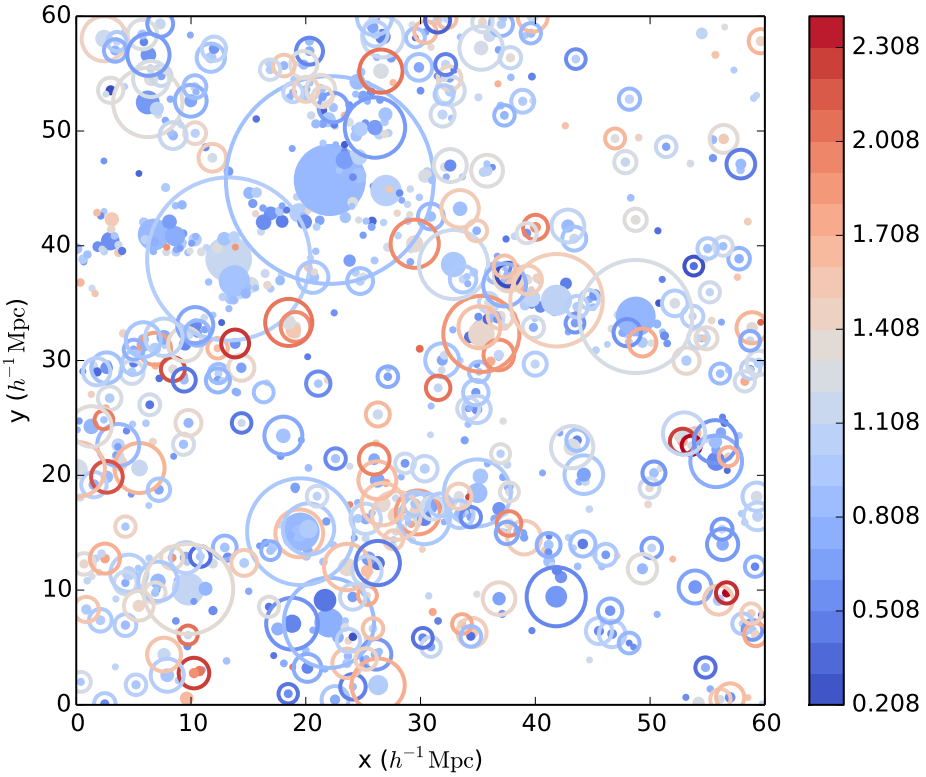

Figure 17. A 20 h^{-1}Mpc deep cut of L0250 along the z-axis. This zoom-in demonstrates the process that decreases the shape parameter as a function of clustering. The size of each circle represents the projection of a spherical dark matter halo with a given halo radius onto the x-y plane. Filled circles use the $\Delta = 200$ catalog and unfilled circles use the $\Delta = 10$ catalog in order to make the effect more visible. Color scale refers to the log shape mark, normalized by halos of the same mass.

which we are including ill-resolved halos potentially into the simulation. Namely, utilizing this mass cut on L0250 data includes halos that do not fit the form of the expected monotonic halo mass-concentration relation. We can determine several facts from this exercise in resolution testing. The first is that the general behavior of the marks seems to be the same regardless of the influence of the resolution effects. Decreasing the value of Δ still moves our marked correlation functions in the same directions as the previous mass cut, although often from a very different starting location. Even with potentially ill resolved objects, the method can be brought to bear upon the problem - potentially a concern if the simulation's ability to resolve a particular statistic is questionable. Also noteable is that the level of the assembly bias is reduced in the case of this lower mass cut in L0250 when compared to L0125. This is distinctly different from our previous example, in which both L0125 and L0250 both contain only well resolved halos within the mass cut and have nearly identical assembly bias at every scale, aside from simulation noise. This seems to imply that including unphysical halos in our sample makes it difficult to determine the actual assembly bias at work.

We can repeat this exercise by looking at a different set of mass cuts. In this case we will utilize our highest mass cut on L0250and L0500. This case does not include poorly resolved halos as we were including in the previous example. Instead, the smaller sized box runs the risk of having less of the most massive halos, resulting in having a larger variance for objects at high mass. The results of this are shown in Figure 24 through Figure 29. There are several key observations to be taken away from this series of plots. The first is the fact that like in our previous example, we see no significant change in assembly bias when only including well resolved halos and see a considerable change when we include unresolved halos in L0500. Of greater import is the fact that we see that in several cases, when interest is only in the most massive halos we find that there is next to no assembly bias. Changing our definition of the halo radius in these cases can even induce halo assembly bias. Given the previous discussion regarding the differences in halo radius definitions chosen (e.g. critical density versus mean density), this implies that we can have very different measurements of this effect solely based on halo definition - a fact that has yet to be explored thoroughly within the literature.

[ARZ: ... AND ELIMINATING ALL THE WAY TO HERE!]

[ARZ: Instead, add one summarizing paragraph here discussing the mass dependence of assembly bias. Emphasize that our findings suggest that the strength of assembly bias can be a strong

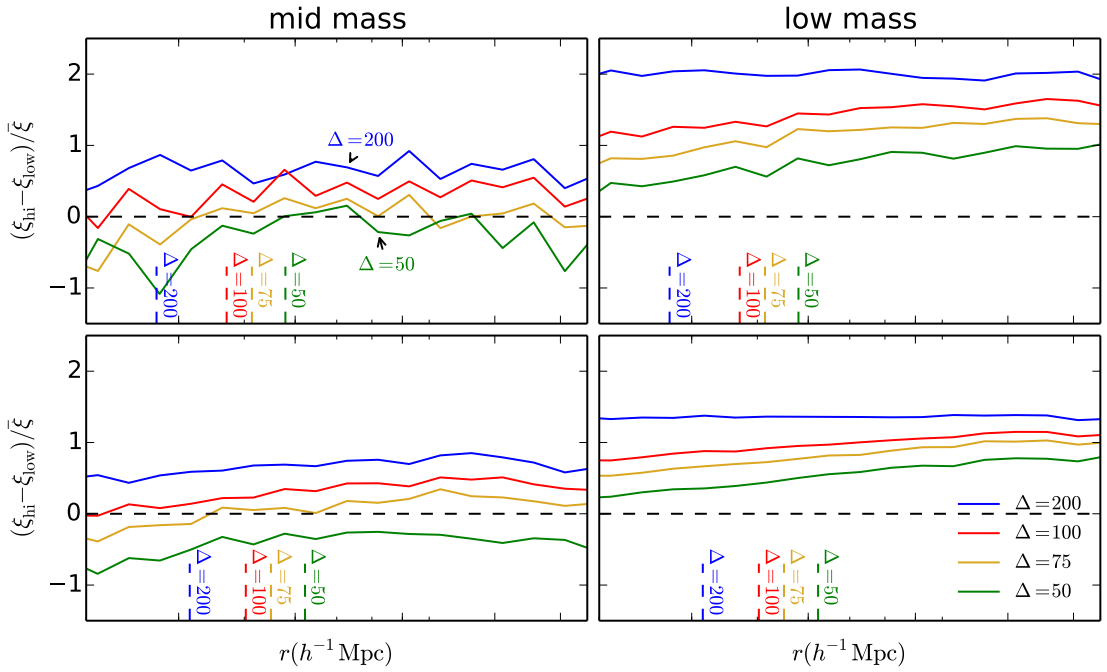

Figure 18. The difference of the correlation function for only the top 20% most concentrated halos and the bottom 20% in concentration, normalized by the overall correlation function of the entire sample. The top row uses L0125 data while the bottom row uses L0250 data. The left column utilizes the "mid mass" cutoff, while the right column demonstrates the "low mass" cutoff. The dashed lines along the bottom denote the largest halo radius for a given value of the overdensity parameter

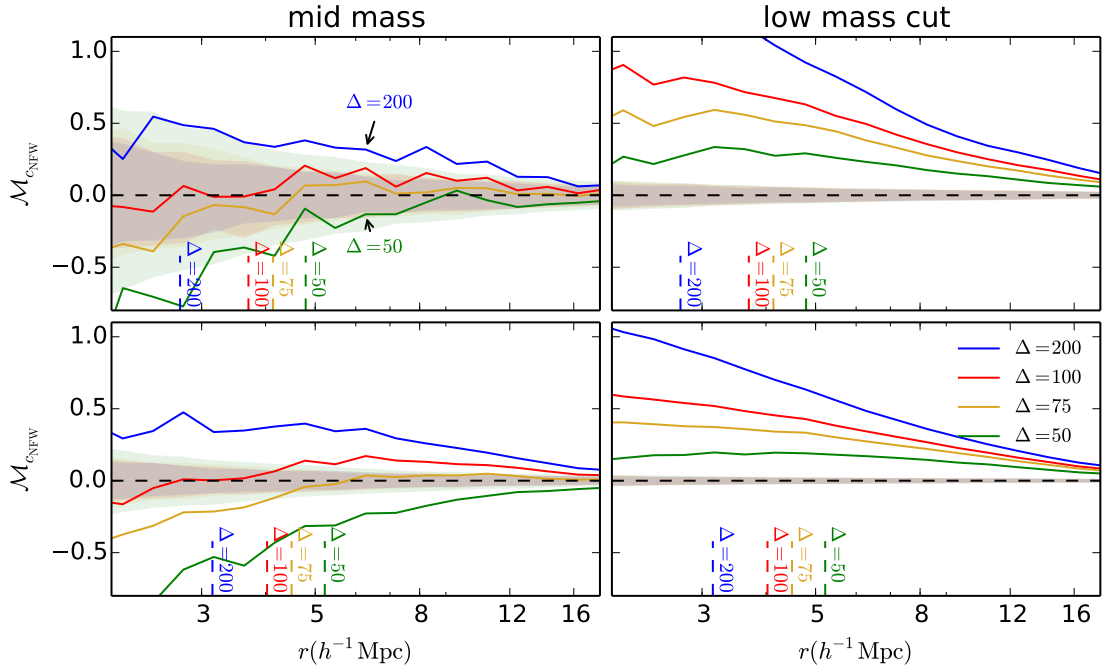

Figure 19. Comparison of the marked correlation function for the concentration defined according to the NFW profile between the "mid mass" cutoff (left column) and the "low mass" cutoff (right column). The top row uses L0125 data while the bottom row uses L0250 data. The shaded bands represent 2-sigma confidence regions generated by randomization of the marks. The dashed lines along the bottom denote the largest halo radius for a given value of the overdensity parameter.

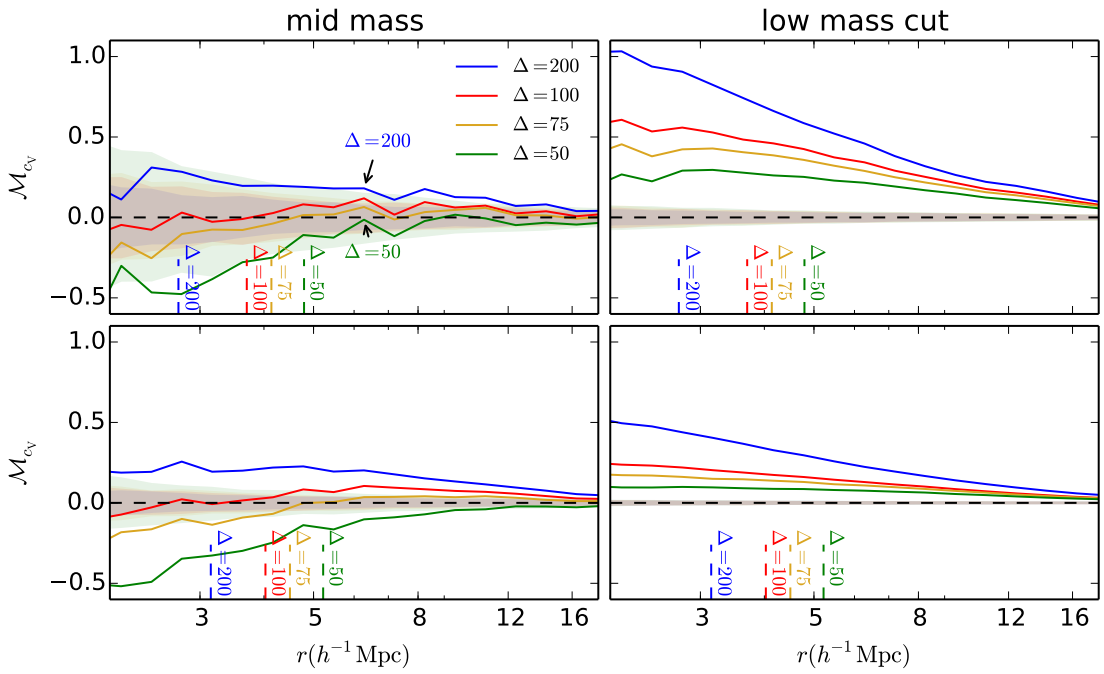

Figure 20. Comparison of the marked correlation function for the concentration defined according to the velocity ratio between the "mid mass" cutoff (left column) and the "low mass" cutoff (right column). The top row uses L0125 data while the bottom row uses L0250 data. The shaded bands represent 2-sigma confidence regions generated by randomization of the marks. The dashed lines along the bottom denote the largest halo radius for a given value of the overdensity parameter.

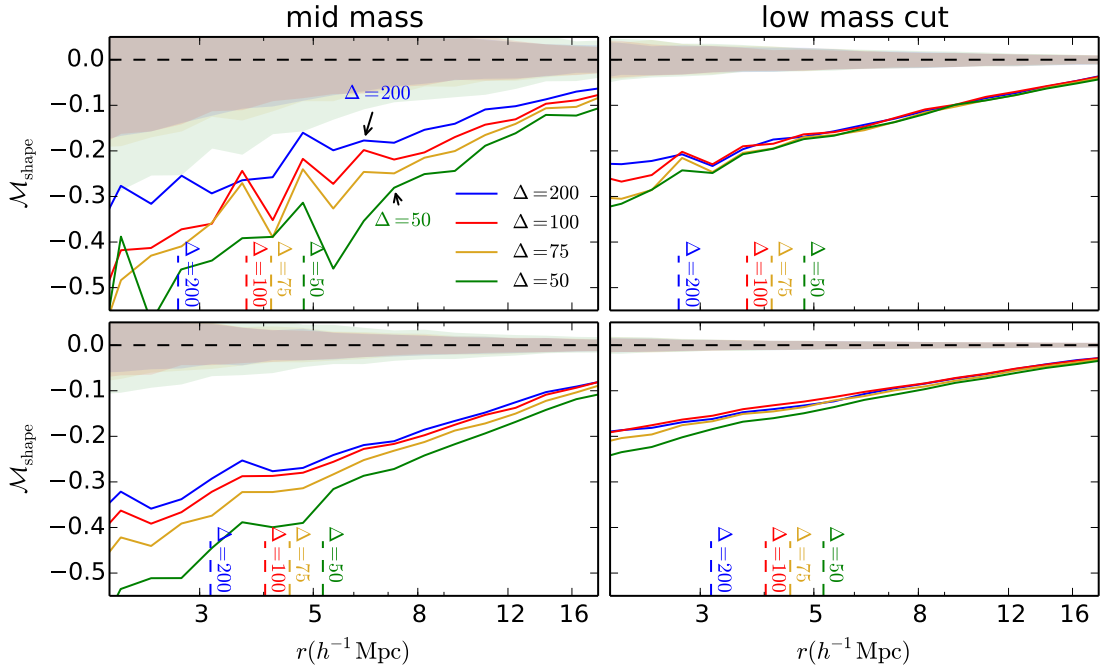

Figure 21. Comparison of the marked correlation function for the shape of the halo between the "mid mass" cutoff (left column) and the "low mass" cutoff (right column). The top row uses L0125 data while the bottom row uses L0250 data. The shaded bands represent 2-sigma confidence regions generated by randomization of the marks. The dashed lines along the bottom denote the largest halo radius for a given value of the overdensity parameter.

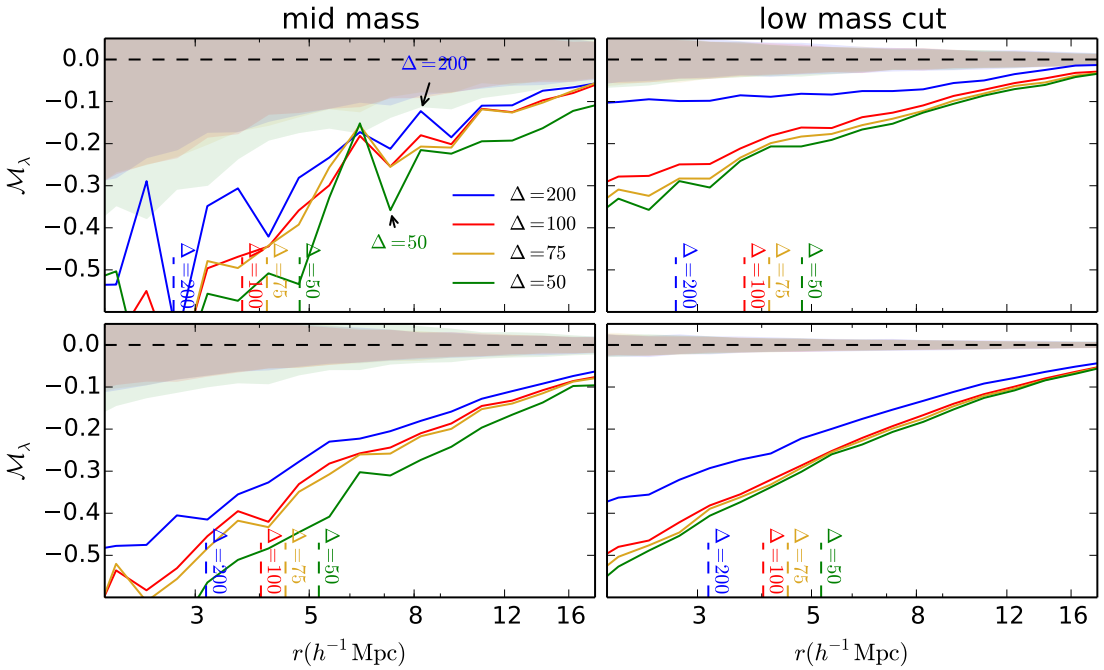

Figure 22. Comparison of the marked correlation function for the spin of the halo between the "mid mass" cutoff (left column) and the "low mass" cutoff (right column). The top row uses L0125 data while the bottom row uses L0250 data. The shaded bands represent 2-sigma confidence regions generated by randomization of the marks. The dashed lines along the bottom denote the largest halo radius for a given value of the overdensity parameter.

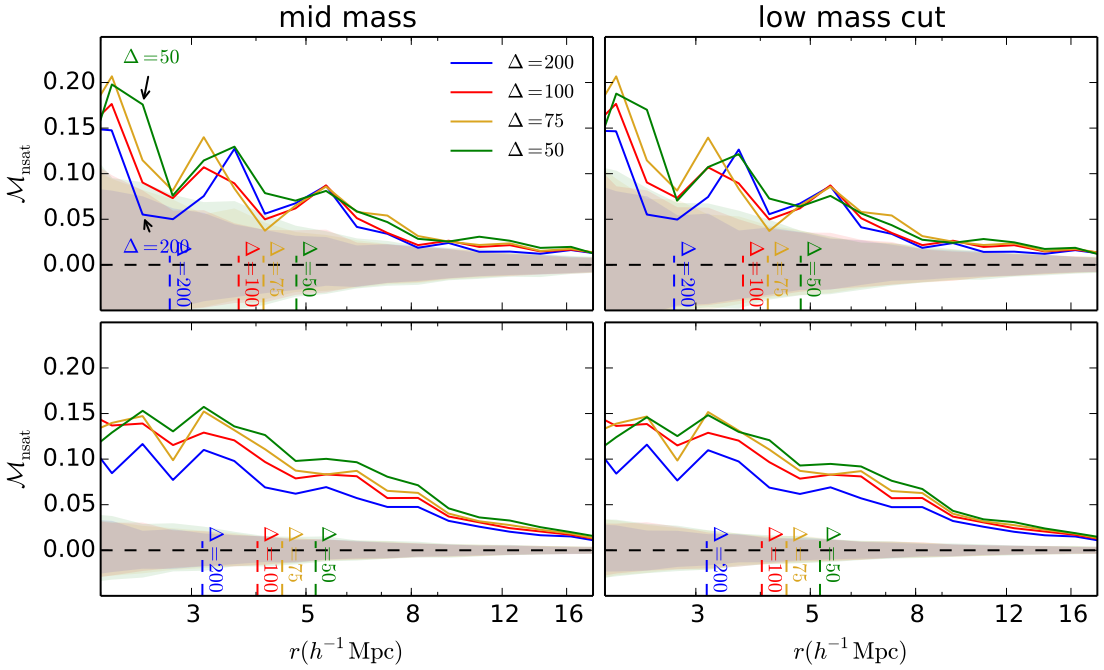

Figure 23. Comparison of the marked correlation function for the satellite number between the "mid mass" cutoff (left column) and the "low mass" cutoff (right column). The top row uses L0125data while the bottom row uses L0250data. The shaded bands represent 2-sigma confidence regions generated by randomization of the marks. The dashed lines along the bottom denote the largest halo radius for a given value of the overdensity parameter.

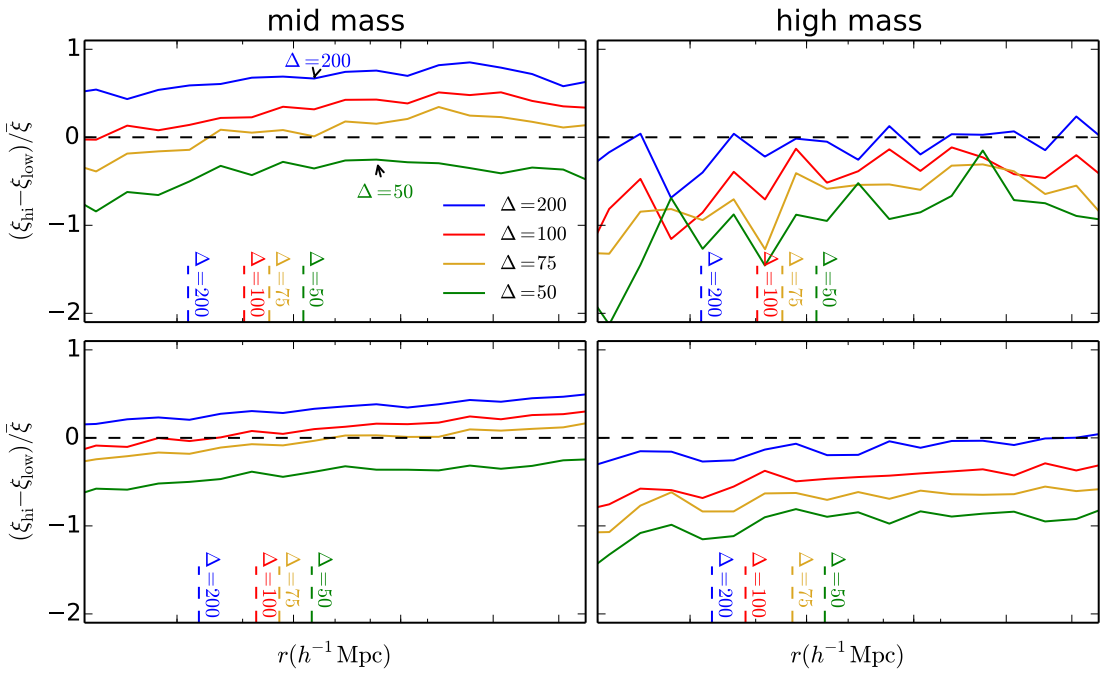

Figure 24. The difference of the correlation function for only the top 20% most concentrated halos and the bottom 20% in concentration, normalized by the overall correlation function of the entire sample. The top row uses L0250 data while the bottom row uses L0500 data. The left column utilizes the "mid mass" cutoff, while the right column demonstrates the "high mass" cutoff. The dashed lines along the bottom denote the largest halo radius for a given value of the overdensity parameter

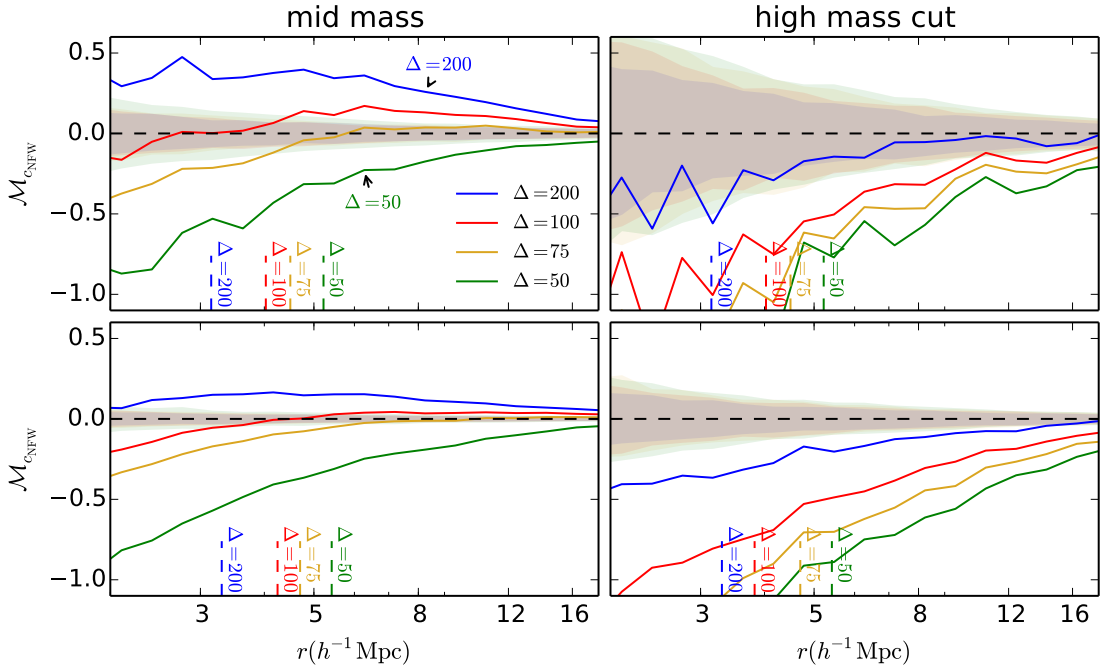

Figure 25. Comparison of the marked correlation function for the concentration defined according to the NFW profile between the "mid mass" cutoff (left column) and the "high mass" cutoff (right column). The top row uses L0250 data while the bottom row uses L0500 data. The shaded bands represent 2-sigma confidence regions generated by randomization of the marks. The dashed lines along the bottom denote the largest halo radius for a given value of the overdensity parameter.

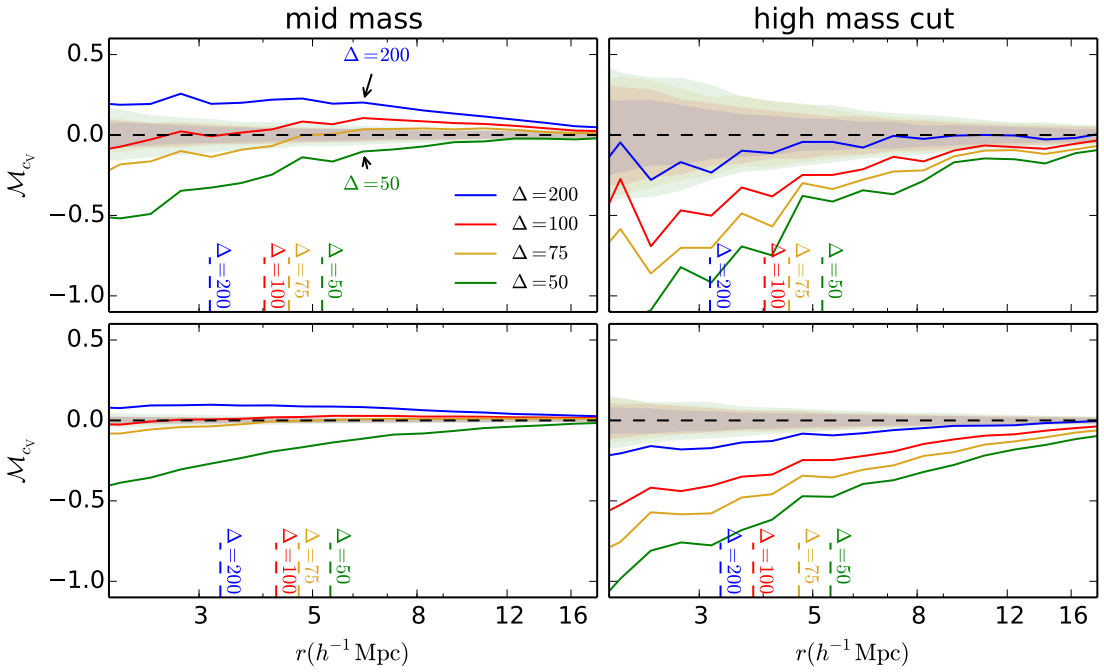

Figure 26. Comparison of the marked correlation function for the concentration defined according to the velocity ratio between the "mid mass" cutoff (left column) and the "high mass" cutoff (right column). The top row uses L0250 data while the bottom row uses L0500 data. The shaded bands represent 2-sigma confidence regions generated by randomization of the marks. The dashed lines along the bottom denote the largest halo radius for a given value of the overdensity parameter.

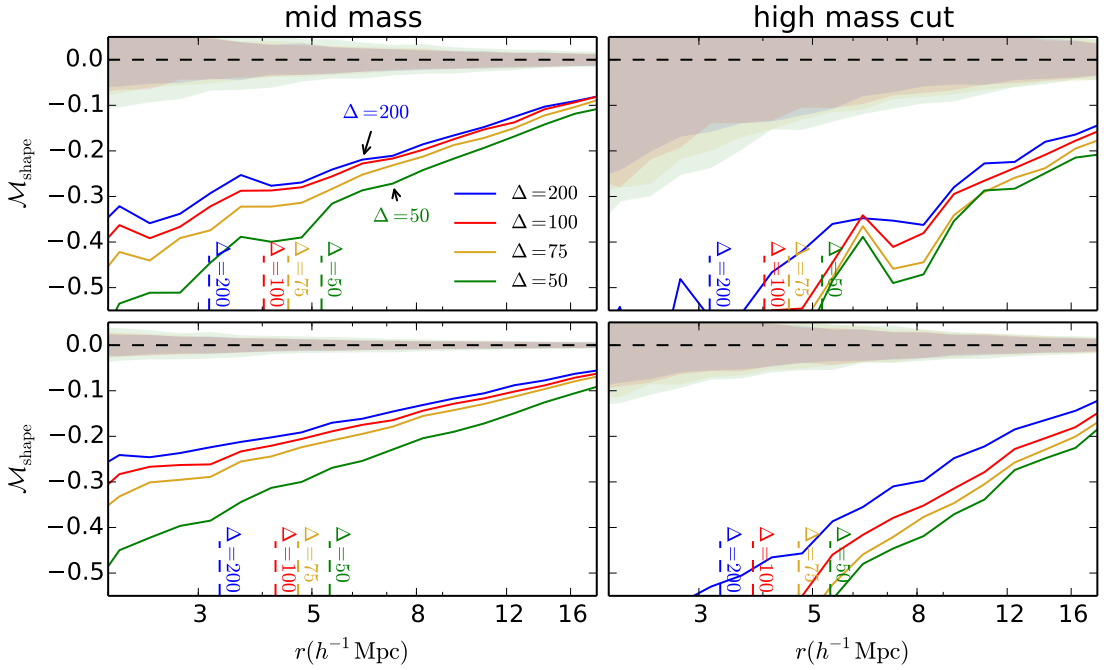

Figure 27. Comparison of the marked correlation function for the shape of the halo between the "mid mass" cutoff (left column) and the "high mass" cutoff (right column). The top row uses L0250 data while the bottom row uses L0500 data. The shaded bands represent 2-sigma confidence regions generated by randomization of the marks. The dashed lines along the bottom denote the largest halo radius for a given value of the overdensity parameter.

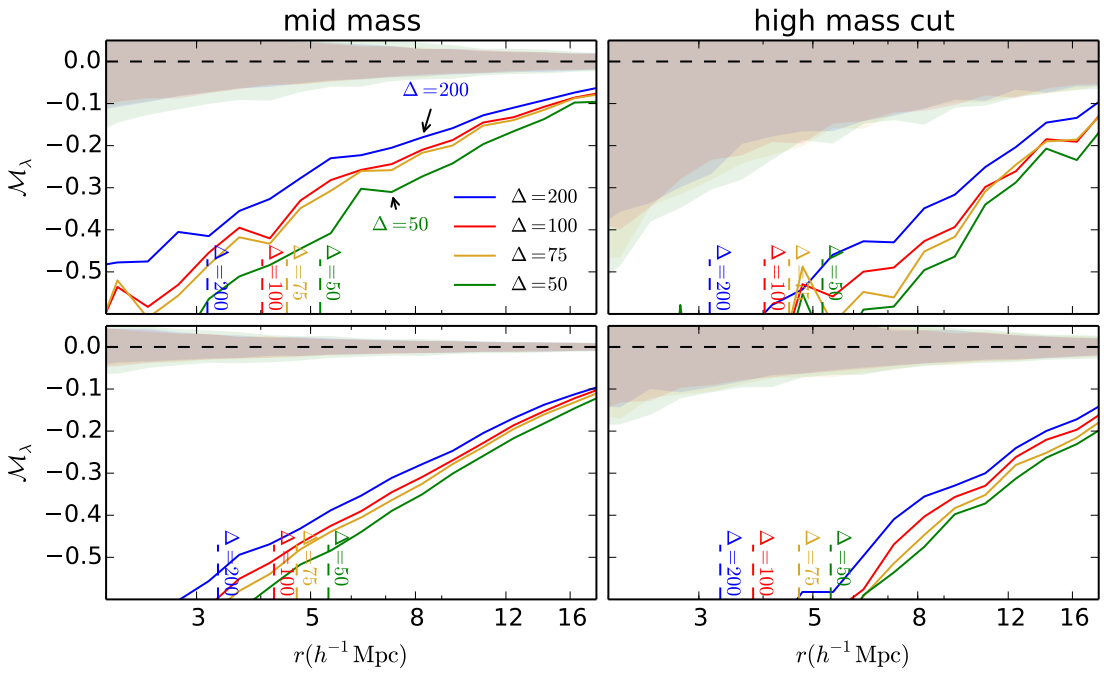

Figure 28. Comparison of the marked correlation function for the spin of the halo between the "mid mass" cutoff (left column) and the "high mass" cutoff (right column). The top row uses L0250 data while the bottom row uses L0500 data. The shaded bands represent 2-sigma confidence regions generated by randomization of the marks. The dashed lines along the bottom denote the largest halo radius for a given value of the overdensity parameter.

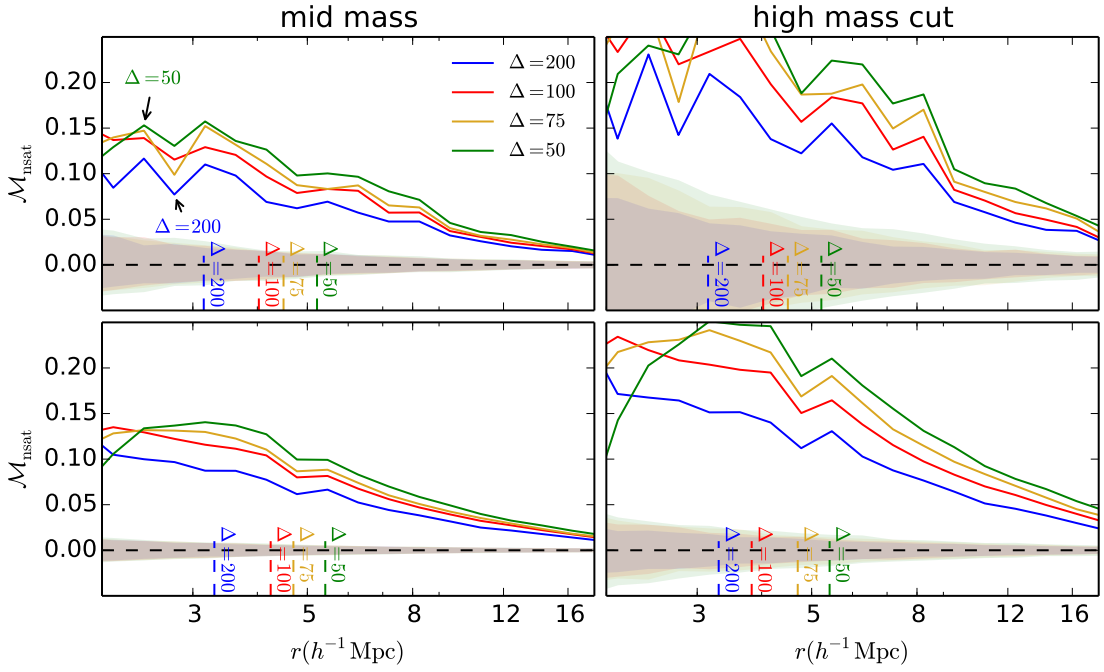

Figure 29. Comparison of the marked correlation function for the satellite number between the "mid mass" cutoff (left column) and the "high mass" cutoff (right column). The top row uses L0250 data while the bottom row uses L0500 data. The shaded bands represent 2-sigma confidence regions generated by randomization of the marks. The dashed lines along the bottom denote the largest halo radius for a given value of the overdensity parameter.

function of halo definition and that this may already be making it difficult to compare the results of various different research groups using different halo definitions.]

7 CONCLUSIONS

[ARZ: After dealing with the comments above, let's come back to rewriting the conclusions section.] We have looked at how to use CFs and MCFs in order to analyze the environmental effects upon the properties of the halo. We have suggested a method of removing the mass dependence that is not subject to the small number statistics at large halo masses. Taking our various tests, we then apply a change to the threshold density Δ in an attempt to remove the effect that environment has upon these properties. We come to the following conclusions from our simulation data.

- Our halo redefinition method does not cause any substantial breakdown in the ROCKSTAR halo finding algorithm, though this may not be the case for every halo finding methodology. This is something that should be considered prior to utilization of this method, unless working directly from particle data. As our initial halo sizes and locations are determined through spherical overdensities, it cannot be assumed that starting from a FoF grouping and then determining values through particle data directly will produce identical results. Similarly, different cosmologies may remove environmental effects at different scales.
- When looking at the two-point correlation function, there appears to be a "sweet spot" that appears to remove environmental effects the most efficiently. Going beyond that seems to reintroduce environmental effects, possibly as an extreme side effect of halo exclusion.
- For our marked correlation functions we see that both proxies of concentration that we use as marks show significant removal of environmental effects at large scales for similar values of the overdensity parameter Δ. In cases where one is only interested in the concentration of dark matter halos and large scales (or correspondingly small values of k), this method will allow you to compensate for bias that environment could introduce to calculations dependent upon the halo model. This may prove valuable for calculations such as that of the shear power spectrum calculated through weak lensing.
- The environmental effects on the shape of the host halo and the satellite number of the host halo cannot be removed regardless of the chosen redefinition of Δ. We propose that this may be intrinsically tied to the nature of the filaments, whose effects cannot be removed by a simple redefinition of the halo radius.
- This method is definitively related to the mass of the halos that are being observed. Furthermore, it appears that the majority of the reduction in assembly bias is tied to the exclusion of halos from the catalog as a result of being subsumed into larger halos. This information does not seem to be contradictory; it can be intuitively understood that the region about the most massive halos will be different than the region around the least massive halos, leading to a different frequency at which halos are being excluded. It does however warrant that careful consideration be given to the sample of halos that are of interest.
- The selection of halo size is intrinsically related to the assembly bias and varies across scales. This might help to resolve contradictory results in the search for halo assembly bias in the literature.

This methodology, while certainly not perfect in accounting for assembly bias, may be of significance when applied to galaxy formation models and give insight into seemingly conflicting results. Provided that the properties of interest in a given model behave well under our redefinition, it will allow us to create better mock galaxy catalogs without resorting to more complicated models requiring halo formation histories - giving us another powerful tool to test observation against.

There remain possible uncertainties to study in the future. One possible area of follow-up is the matter of simulation cosmology, which is not explored in this text. It is possible that the choice of cosmology may change observed assembly bias as a function of the halo masses, something that our methodology should be capable of observing. Furthermore, we can determine if the choice of halo size that best reduces assembly bias is a function of the chosen cosmology. This may be of interest in attempting to determine signatures of assembly bias in observational samples in the future.

ACKNOWLEDGMENTS

We are grateful to many people.

REFERENCES

Allgood B., Flores R. A., Primack J. R., Kravtsov A. V., Wechsler R. H., Faltenbacher A., Bullock J. S., 2006, MNRAS , 367, 1781
Behroozi P. S., Wechsler R. H., Wu H.-Y., 2013, Astrophys. J. , 762, 109
Berlind A. A., Weinberg D. H., 2002, Astrophys. J. , 575, 587
Blumenthal G. R., Faber S. M., Primack J. R., Rees M. J., 1984, Nature , 311, 517
Bond J. R., Cole S., Efstathiou G., Kaiser N., 1991, Astrophys. J. , 379, 440
Bullock J. S., Wechsler R. H., Somerville R. S., 2002, MNRAS , 329, 246
Cooray A., Sheth R., 2002, Phys. Rep., 372, 1
Croton D. J., Gao L., White S. D. M., 2007, MNRAS , 374, 1303
Dalal N., White M., Bond J. R., Shirokov A., 2008, Astrophys. J. , 687, 12
Diemer B., Kravtsov A. V., 2015, Astrophys. J. , 799, 108
Duffy A. R., Schaye J., Kay S. T., Dalla Vecchia C., 2008, MNRAS , 390, L64
Dvorkin I., Rephaeli Y., 2011, MNRAS , 412, 665
Gao L., White S. D. M., Jenkins A., Frenk C. S., Springel V., 2005, MNRAS , 363, 379

Gil-Marín H., Jimenez R., Verde L., 2011, MNRAS , 414, 1207
Harker G., Cole S., Helly J., Frenk C., Jenkins A., 2006, MNRAS , 367, 1039
Kazantzidis S., Zentner A. R., Kravtsov A. V., 2006, Astrophys. J. , 641, 647
Lacey C., Cole S., 1993, MNRAS , 262, 627
Navarro J. F., Frenk C. S., White S. D. M., 1997, Astrophys. J. , 490, 493
Peacock J. A., Smith R. E., 2000, MNRAS , 318, 1144
Peebles P. J. E., 1969, Astrophys. J. , 155, 393
Scoccimarro R., Sheth R. K., Hui L., Jain B., 2001, Astrophys. J. , 546, 20
Seljak U., 2000, MNRAS , 318, 203
Sheth R. K., Tormen G., 2004, MNRAS , 350, 1385
Somerville R. S., Kolatt T. S., 1999, MNRAS , 305, 1
Tempel E., Guo Q., Kipper R., Libeskind N. I., 2015, ArXiv e-prints
Velliscig M., Cacciato M., Schaye J., Bower R. G., Crain R. A., van Daalen M. P., Dalla Vecchia C., Frenk C. S., Furlong M., McCarthy I. G., Schaller M., Theuns T., 2015, ArXiv e-prints
Wechsler R. H., Bullock J. S., Primack J. R., Kravtsov A. V., Dekel A., 2002, Astrophys. J. , 568, 52
Wechsler R. H., Zentner A. R., Bullock J. S., Kravtsov A. V., Allgood B., 2006, Astrophys. J. , 652, 71
White S. D. M., Rees M. J., 1978, MNRAS , 183, 341
Zentner A. R., 2007, International Journal of Modern Physics D, 16, 763
Zentner A. R., Berlind A. A., Bullock J. S., Kravtsov A. V., Wechsler R. H., 2005, Astrophys. J. , 624, 505

APPENDIX

One natural question that might arise in the analysis of this work is the nature of the resulting assembly bias trends. Our focus in the main sections of this paper is on the nature of the assembly bias changing as a function of the mass cut chosen. Our conclusions include the fact that there is a strong mass dependence on halo assembly bias that must be accounted for seperately depending on the halos of interest in a study. However, while the existence of this trend is clear within our analysis, the determination that this is solely due to the masses of the halos included in our calculation is less clear upon closer inspection. One possibility that might be particularly concerning is the potential that the different simulations have created halos that have fundamentally different clustering and this is leading to the result that we are interpreting as a mass dependence on assembly bias. Thankfully, though our statistics become less meaningful to carry out this calculation, we can carry out a comparison using the same mass cut across two of our simulations, knowing that these will only contain well resolved halos.

While not addressed directly, Figure 18 through Figure 23 contain a demonstration of the result that we are seeking in the left column of panels. The lower left panels show various marks of interest for L0250 using the "mid mass" cut on the data set. In comparison, the upper left panel contains the same marks of interest for the L0125 using the same mass cut. In the latter, there are fewer halos in this mass cut range, as a result of the smaller simulation box size. However, we note that despite the additional noise in the data set, the behavior of the assembly bias measurement is nearly identical within tolerances accounting for differences between simulations and noise. This motivates our conclusion that the driver behind the behavior is the mass cut of the data sets rather than the resolution of the simulation.